Solar PV and battery storage feasibility integration in Africa - Taking Djerba as a case study

Alexander Haddad

Thesis submitted for the degree of
Master in Renewable Energy Systems
30 credits

Department of Technology Systems
Faculty of mathematics and natural sciences

UNIVERSITY OF OSLO

May 2024

Solar PV and battery storage feasibility integration in Africa - Taking Djerba as a case study

Alexander Haddad

Solar PV and battery storage feasibility integration in Africa - Taking Djerba as a case study

http://www.duo.uio.no/

Printed: Reprosentralen, University of Oslo

Acknowledgements

I would like to share my gratitude towards my internal supervisor Josef Noll, who have given me insightful feedback and great support throughout this thesis. Additionally, I would like to thank my friends, family and partner for the unconditional support and help for the last six months. Also, a big thank you to my two fellow students who have been with me though thick and thin, and whom I have shared the ups and downs with.

Thank you all!

Abstract

Renewable energy sources have witnessed significant growth and exploitation in recent years, driven by policies, incentives, and investments aimed at combating climate change and reducing global greenhouse gas emissions. Despite these positive developments, the goal of reaching net zero by 2050 remains elusive, particularly in rural areas like Africa, where reliance on fossil fuel-based energy sources persists. Challenges such as inadequate infrastructure, political differences, limited electricity access, and economic insecurities have impeded progress, making Africa one of the continents lagging in renewable energy adoption. This thesis investigates the feasibility of integrating an off-grid solar photovoltaic (PV) energy system with battery storage in Africa, using the island of Djerba in Tunisia as a case study. Djerba, located near the equator, benefits from excellent solar potential and stable sunlight throughout the year, making it an ideal candidate for solar PV integration as an alternative to fossil fuel-based power plants. The proposed energy system model includes up to 473 MW of solar PV capacity and 556 MWh of battery storage, generating a total of 170 GWh of electricity annually. The implementation of this system has demonstrated significant benefits, including a 56% contribution to Djerba's total electricity demand and a reduction of CO emissions by 40% annually. The total system cost is estimated at 1.5 B$, with a levelized cost of electricity (LCOE) of 228 $/MWh. Despite these promising findings, the actual deployment of this proposed system faces economic and political challenges. The successful implementation of large-scale solar PV systems in Africa is contingent upon securing robust funding and international investment. In conclusion, while solar PV systems hold great potential for sustainable energy in Africa, addressing the economic and political barriers is crucial for their widespread adoption and contribution to the global fight against climate change.

Contents

Acknowledgements **i**

Abtract **ii**

1 Introduction **1**
1.1 Background 1
1.2 Motivation 2
1.3 Scope of work 2
1.4 Problem definition 3
1.5 Thesis structure 3

2 Case study **4**
2.1 Overview of Tunisia 4
2.1.1 General information 4
2.1.2 Climate and topology 5
2.1.3 Energy mix 6
2.1.4 Power sector 7
2.1.5 Current and future plans 7
2.1.6 Challenges 8
2.2 Overview of Djerba 9
2.2.1 Energy mix 9
2.2.2 Challenges 10

3 Theoretical background **11**
3.1 Solar Energy 11
3.1.1 Solar radiation 11
3.1.2 Atmospheric effects 12
3.1.3 Air mass 13
3.1.4 Irradiation components 13
3.1.5 Standard Test Conditions 14
3.1.6 Solar resource data available 14
3.1.7 Solar generation 15
3.2 Battery storage 15
3.2.1 Key metrics 16
3.2.2 Battery efficiency 16
3.2.3 Capacity 17

3.2.4 Comparison of battery characteristics . . . 17
3.2.5 Battery equations . . . 17
3.3 Financial metrics . . . 18
3.4 Literature review . . . 19
3.4.1 PV uptake in North Africa . . . 19
3.4.2 RES powered water desalination plant . . . 20
3.4.3 Modeling a solar PV system . . . 22
3.4.4 Modeling tools . . . 24
3.4.5 Summary of literature . . . 24

4 Data collection and pre-processing **27**
4.1 Solar resource assessment . . . 27
4.2 Electricity demand . . . 29
4.2.1 Water desalination plant . . . 29
4.2.2 Residential sector . . . 32
4.2.3 Hotel sector . . . 33

5 Model development and set up **35**
5.1 Land availability . . . 35
5.2 Energy system layout . . . 35
5.2.1 Technical inputs . . . 38
5.2.2 Economic inputs . . . 39
5.3 Building optimization model . . . 40
5.3.1 Set definition . . . 40
5.3.2 Objective Function . . . 40
5.3.3 Constraints . . . 40
5.3.4 Parameters . . . 40
5.3.5 Variables . . . 41
5.3.6 Equations . . . 41

6 Evaluation of the results **42**
6.1 Visualisation of the results . . . 42
6.1.1 System Architecture . . . 42
6.1.2 Solar resource . . . 43
6.1.3 Base case scenario . . . 44
6.1.4 Scenario 1 . . . 46
6.1.5 Scenario 2 . . . 48

7 Conclusion **52**

A Appendix: Consumption data **59**

List of Figures

2.1 Tunisia on a map [14] 5
2.2 Map overview with GHI and PV power potential in 2023 [12] 6
2.3 Share of renewable energy sources 2021 (in %) - own illustration [28] . 7
2.4 Djerba location in Tunisia [13] 9

3.1 Geometrical constants for finding the Earth's solar irradiance[24] . . . 12
3.2 Irradiation components and how they shed light on a solar panel β . . 14

4.1 Solar irradiation for a year from PVGIS 28
4.2 Ambient temperature from PVGIS 28
4.3 Yearly electricity consumption of the water desalination plant 30
4.4 Summer and winter daily electricity consumption profiles 31
4.5 Daily water consumption profile 32
4.6 Electric load profile in the residential sector 33
4.7 Electric load daily profile for the hotel sector 34

5.1 Energy system illustration 36
5.2 Flow chart of the simulation steps 38

6.1 Yearly global tilted irradiance (W/m^2) 43
6.2 Daily summer vs winter global tilted irradiance (W/m^2) 44
6.3 Solar PV generation and battery behaviour for a summer day 45
6.4 Solar PV generation and battery behaviour results from scenario 1 - summer day 47
6.5 Solar PV generation and battery behaviour results from scenario 1 - winter day 48
6.6 Solar PV generation and battery behaviour from Scenario 2 - summer day 49
6.7 Solar PV generation and battery behaviour for scenario 2 - winter day 50

List of Tables

3.1 Comparison of Battery Characteristics 17
3.2 Solar PV Costs in Africa 20
3.3 Technical and economic parameters from papers 26

4.1 Monthly and yearly total electricity consumption of the desalination plant in GWh (2023) A 30
4.2 Values of parameters for water consumption model [38] 31

5.1 Technical inputs for the system 39
5.2 Economic inputs for the system 39

6.1 Parameter output results for a summer day 45
6.2 Parameter output results for a winter day 46
6.3 Parameter output results for scenario 1 - summer day 47
6.4 Parameter output results for scenario 1 - winter day 48
6.5 Parameter outputs results for scenario 2 - summer day 49
6.6 Parameter output results for scenario 2 - winter day 50

Chapter 1

Introduction

1.1 Background

The rate of global warming is increasing, with temperatures reaching historically high levels. This rapid change is affecting the climate, leading to extreme weather disasters across the globe [47]. In response, international frameworks such as the Paris Agreement, National Adaptation Plans, and Nationally Determined Contributions (NDCs) have been established to mitigate the most severe impacts of this climate crisis. These agreements aim to limit global temperature increases to no more than 1.5°C above pre-industrial levels [54]. Achieving this threshold requires a a 42% reduction in greenhouse gas (GHG) emissions by 2030 along with an ambitious goal of achieving net zero emissions by 2050 [47].

One of the major contributors to the GHG emissions, is the energy sector. It is responsible for more than three-quarters of the total emissions worldwide. This contribution exceeds that of other sectors such as transportation, agriculture, and industry [31]. This highlights the significant impact of energy consumption and production patterns on global emissions. Changing these energy behaviors is essential, and substantial reductions in this sector are necessary to achieve international climate goals.

The transition from fossil fuel based energy sources to a greener, more sustainable energy landscape has increased in the recent years, supported by policy initiatives and reductions in costs. In 2023, the clean energy sector experienced significant growth, with solar PV and wind energy capacities increasing by 85% and 60%, respectively, achieving a total installed capacity of nearly 540 GW. Investments in the clean energy sector increased by almost 50% compared to 2019, reaching $1.8 trillion, highlighting the global shift to renewable energy. However, this deployment was mainly concentrated in advanced economies and China, which together accounted for 90% of the capacity increases that year. [32]

Despite these global advances in the green energy transition, Africa remains a unique case. This resource rich continent has vast, yet largely unused, potential for renewable energy sources such as solar, wind, and hydro. These resources have a great potential to improve the energy supply while meeting local energy demands. However, Africa faces significant challenges, including political, economic, and demographic difficulties. Worsened by inadequate infrastructure, these issues prevent widespread access to electricity and clean water, highlighting the critical need for integrated energy solutions. [35]

1.2 Motivation

This thesis aims to investigate the possibilities of integrating solar PV generation with energy storage on the African continent. Djerba island, located in southeastern Tunisia, serves as an insightful case study for exploring the possibilities associated with stand alone solar energy system deployment in Africa.

The main motivation for this research is driven by a combination of academic interests and personal connections to Africa, particularly Tunisia. Having spent eleven years living in the country, I have developed great interest for the possibilities of implementing renewable energy sources in undeveloped areas. The personal experience linked with living across the European boarders has given me a different perspective on the region's challenges and opportunities.

This study tends to shed light on Tunisia and Djerba's energy consumption and production, while investigating the integration of solar PV with energy storage. While it may be optimistic to expect this research to revolutionize the complex energy issues related to Tunisia, I believe it will contribute to considerable insights that can help advancing towards global sustainability goals.

1.3 Scope of work

The primary objective of this study is to determine the feasibility of integrating an energy system with solar PV and energy storage. This combination can serve as a good alternative for traditional fossil fuel based systems, especially in island. This integration will be developed through an optimization model aimed at determining the feasibility of this system based on a technical and economic point of view.

The following steps will be undertaken in order to achieve the goal of this study:

- Literature review on solar PV solutions and battery systems
- Deciding necessary parameters involved in process as such
- Data collection and processing using Python program
- Development of the energy system using GAMS tool based on data and assumptions
- Evaluate the energy system based on the following scenarios
  - Base case: Solar PV with battery storage with load from the water desalination plant

- Base case augmented with load from the residential sector

- Conclude the feasibility of the system

1.4 Problem definition

The following research questions are decided:

RQ 1. What is the current state of solar PV technology?

RQ 2. How is the climate, topology, energy behaviour etc of Djerba Island?

RQ 3. What parameters should be included in the modeling analysis from a techno-economic perspective?

RQ 4. How can modeling results for specific applications be evaluated in terms of future scalability?

1.5 Thesis structure

Case study
This part of the study provides an overview of Tunisia and the island of Djerba.

Theoretical background
This section establishes the theoretical framework of the thesis, describing PV system, battery specifics and a review of the current state of the art.

Data collection and pre-processing Necessary data such as weather and demand are both obtained and generated. This section describes this process.

Model development and set up
This chapter details the modeling approach based on the main findings from the literature, as well as the methods and tools used.

Evaluation of the results
This chapter evaluates the modelling set up, the optimization problem of the base case scenario and identifies the outcome of this process.

Conclusion
The final section sums up the work and suggest future research and potential developments in this field of study.

Chapter 2

Case study

This part of the study provides a general overview of Tunisia along with a more detailed explanation of the specific location in question.

2.1 Overview of Tunisia

2.1.1 General information

Tunisia is located in the Maghreb region of North Africa, as shown in Figure 2.1. With a surface area of about 164.000 km^2, it is the smallest country in the region [40]. In 2021, 12 million people inhabited the country, and Tunis, the capital, is considered to be the largest city and the economic hub of the country [55].

Tunisia's economy consists of various sectors where agriculture, manufacturing and tourism play significant roles. However, Tunisia faces challenges such as high unemployment and differences in income and development between different regions. This may have a direct correlation with the Jasmine revolution in 2011 that put an end to the dictatorship regimes that have been ruling the country for more than 30 years. [40]

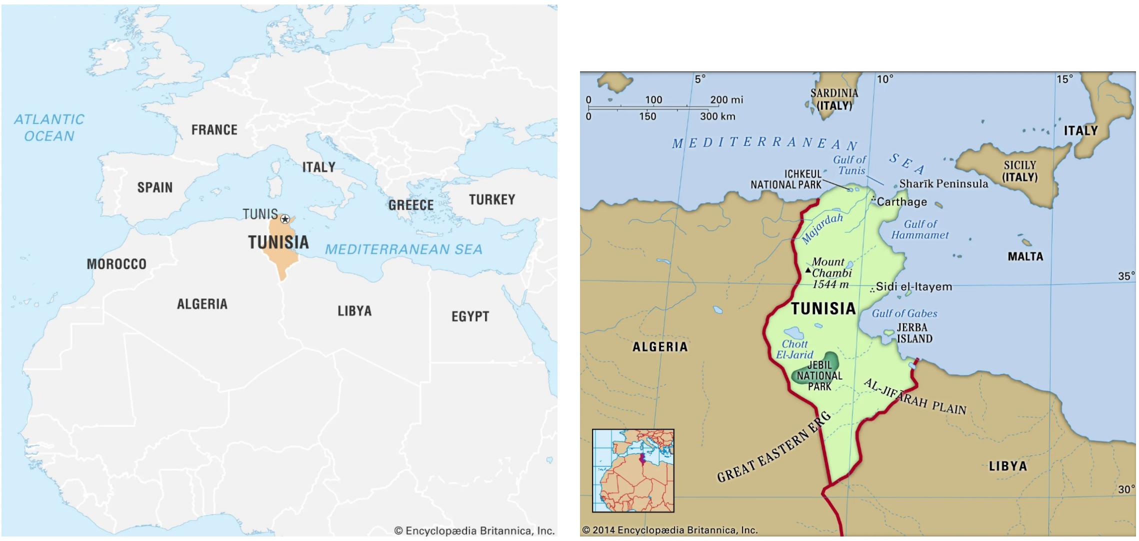

(a) In the World (b) Zoomed in

Figure 2.1: Tunisia on a map [14]

2.1.2 Climate and topology

The country consists of different climate factors, predominantly featuring a Mediterranean climate in the north, a semi-arid climate in the central regions, and a more arid, desert-affected conditions in the south [40]. The global horizontal irradiation varies across the country from north to south, as shown in Figure 2.2a, which indicates the distribution of sunshine hours by region. This variation in irradiation is proportional to the potential for solar PV in the country, as illustrated in Figure 2.2b. According to [56], Tunisia has great renewable energy potential, especially wind energy in the north and central regions, and solar energy in the south. The article further highlights that the country experiences high solar irradiance, ranging from 1800 kWh/m^2/year in the north to 2600 kWh/m^2/year in the south, as indicated in Figure 2.2b. On average, Tunisia has over 3000 hours of sunshine per year, with most southern areas receiving more than 3200 hours and peaks of up to 3400 hours per year in the Gulf of Gabès [7]. Thus, the average global horizontal irradiation ranges between 4.2 kWh/m^2/day and 5.8 kWh/m^2/day. These favorable conditions can contribute to the high productivity of solar PV systems in Tunisia, which can potentially achieve up to 18320 kWh/kWp in the southeast [7].

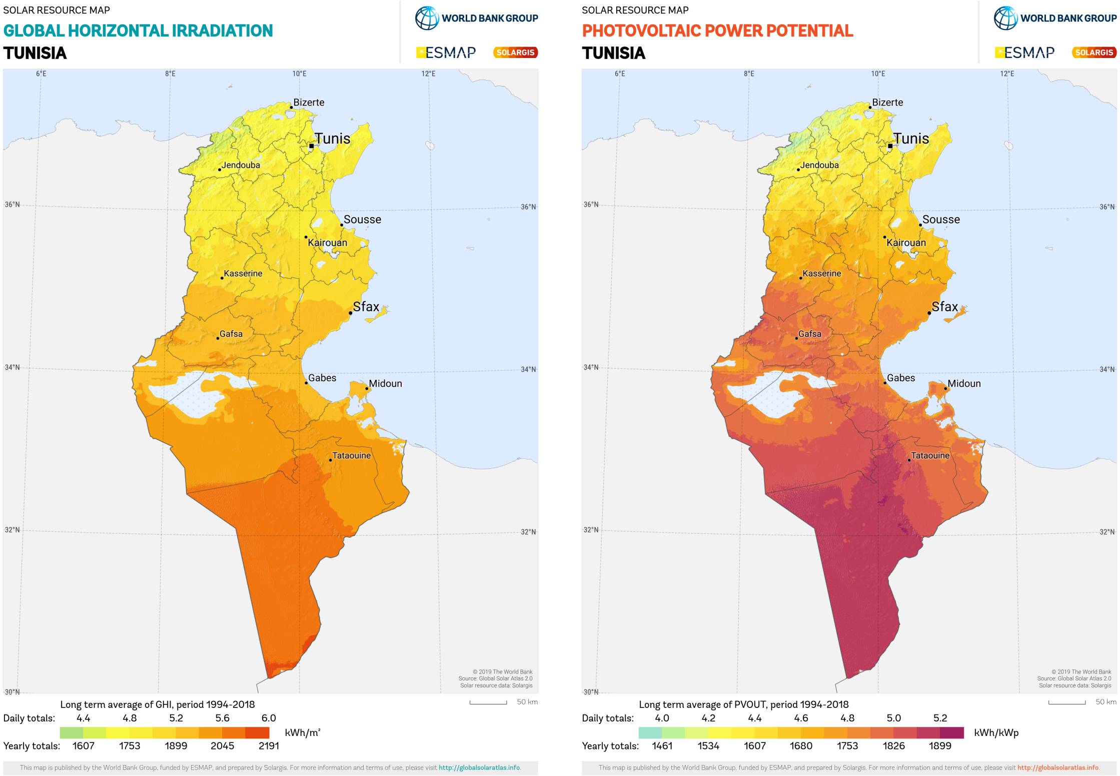

(a) GHI

(b) PV power potential

Figure 2.2: Map overview with GHI and PV power potential in 2023 [12]

2.1.3 Energy mix

Like many African countries, Tunisia remains heavily on fossil fuels, such as natural gas and oil, to meet its primary energy needs. According to the International Energy Association, as of 2021, roughly 90% of the total energy supply was derived from fossil fuels, 9% from biofuels and waste, and the remaining 1% from renewable energy sources (hydro, wind, and solar); with 53% of the total energy supply being imported [29].

The total power production from the Tunisian electricity grid accounted for 22142GWh in 2023 [30]. Around 97% of the total electricity generation is derived from fossil fuels, with 45% of the natural gas being imported from neighboring country Algeria [19]. The remaining 3% electricity generation comes from renewable energy sources. Since the 2000s, renewable energy sources have experienced a significant increase, with a rise of 287% rise in total electricity generation of total electricity generation. [28].

The total share of different renewable energy sources are illustrated in Figure 2.3. Solar PV accounts for the majority of the share, followed by wind and a small amount of hydro power.

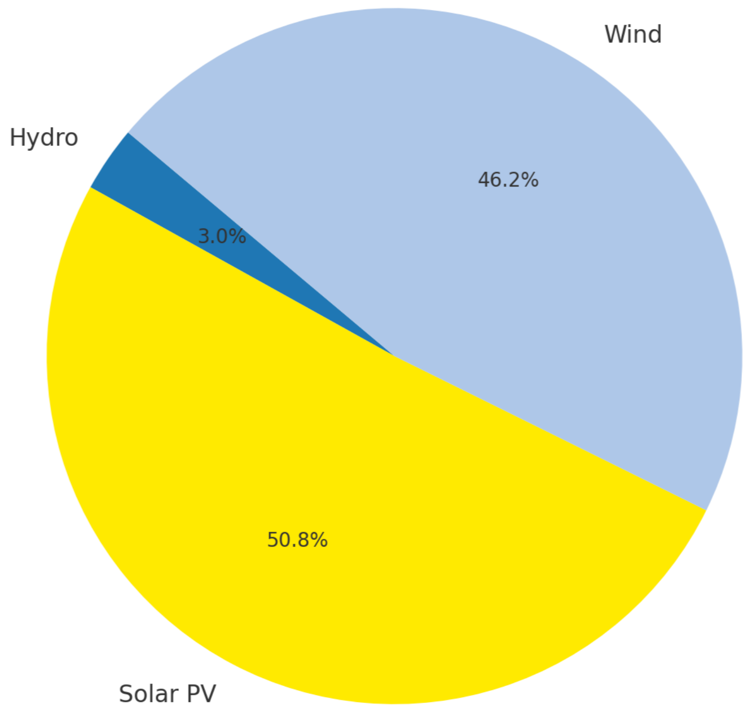

Figure 2.3: Share of renewable energy sources 2021 (in %) - own illustration [28]

2.1.4 Power sector

The country's power sector is mainly owned by state power utility, Société Tunisienne de l'Électricité et du Gaz (STEG), which controls 91% of the electricity production and distribution, while independent power producers (IPPs) contribute to the remaining 9%. [53], [19]. The energy sector has decreased by 4% per year, while demand has grown continously by 2% annually between 2010 and 2021 [19]. The demand is expected to grow by 2% to 5% annually, highlighting the increasing energy needs of the nation [53].

To address financial challenges that the country is facing, several reforms have been implemented since 2014. These reforms include adjustments to power sector subsidies, such as changing tariffs and financial allocations to the the Tunisian company of Electricity and Gas (STEG). These subsidies resulted in significant decreases. Additionally, the government has increased retail tariffs multiple times in recent years to align with global price changes and currency fluctuations. These initiatives are part of Tunisia's strategy to stabilize the energy sector and reduce reliance on subsidized energy while transitioning towards more sustainable energy. [53]

2.1.5 Current and future plans

To reduce reliance on imported energy and to increase sustainability, Tunisia has committed to expanding its renewable energy capacity as part of its broader strategy. The country's goals is to achieve a 30% share from renewable sources in its electricity mix by 2030, in line with the Tunisian Solar Plan (2009) that was initiated in 2009. This plan includes substantial contributions from solar PV systems, solar water heating systems, and wind energy.[20]

The current renewable-based installed capacity includes 244 MW from wind energy. There are several wind farms in the country including a 54 MW wind energy plant in Sidi Daoud, commissioned in 2009, and a 120 MW capacity plant in Bizerte, commissioned in 2012. The solar capacity valued at 15 MW at the end of 2014, mostly from small-sclae private installations. Despite significant private sector interest, there have been no private-sector owned utility-scale renewable energy projects to date. [53]

In 2017, Tunisia started a bidding process for 210 MW of renewable energy, to be built under a build-own-operate model with STEG buying the power. This was part of efforts to promote renewable energy, including feed-in tariffs and a 2018 action plan to speed up renewable energy projects, with plans for another 800 MW. By 2030, Tunisia aims to invest heavily in renewable energy, targeting 940 MW for wind power and 835 MW for solar PV. [53]

The PROSOL program, launched in 2005, is another pivotal initiative, promoting solar energy through financial and fiscal support. It provides loans for domestic customers to purchase solar water heaters and a government subsidy covering 20% of system costs. By 2030, PROSOL aims to install approximately 2.5 million m^2 of solar water heating capacity, generating significant employment opportunities and reducing greenhouse gas emissions.[20]

Further to this, Tunisia's energy strategy includes the ELMED project, which involves constructing a 400 kV submarine cable interconnecting Tunisia and Italy, and aims to reduce primary energy consumption by 30% compared to the business-as-usual scenario by 2030. Carbon intensity is also expected to be cut by 41% by 2030 compared to 2010 levels.[20]

2.1.6 Challenges

Tunisia faces several challenges in its energy sector, including issues with policies and regulations, unstable rules and a monopoly in the energy market. These problems make it hard for international investors to invest in Tunisia. Political instability also discourages foreign investments. The focus on private profit over public interest has led to energy expansion rather than a shift to renewable energy. Reforming the energy system to rely more on renewable sources is a priority for the country. The goals are to attract foreign investments and reduce energy dependence, but achieving a successful energy transition depends on political stability, social equality and political freedom.[19]

2.2 Overview of Djerba

Djerba Island is located just off the southeast coast of Tunisia, in the Gulf of Gabès, as shown in Figure 2.4. The island covers a surface area of 517 km^2 and has a population of roughly 160,000 residents, where 65,000 living in its largest town, Houmt-Sook. [20].

The economy of the island is heavily based on Tourism. Around one million tourists visit the island each year, which provides around 14000 seasonal jobs for its residents. Due to the high touristy activity, the island has about 100 hotels, covering about 45 km of the coast. [20]

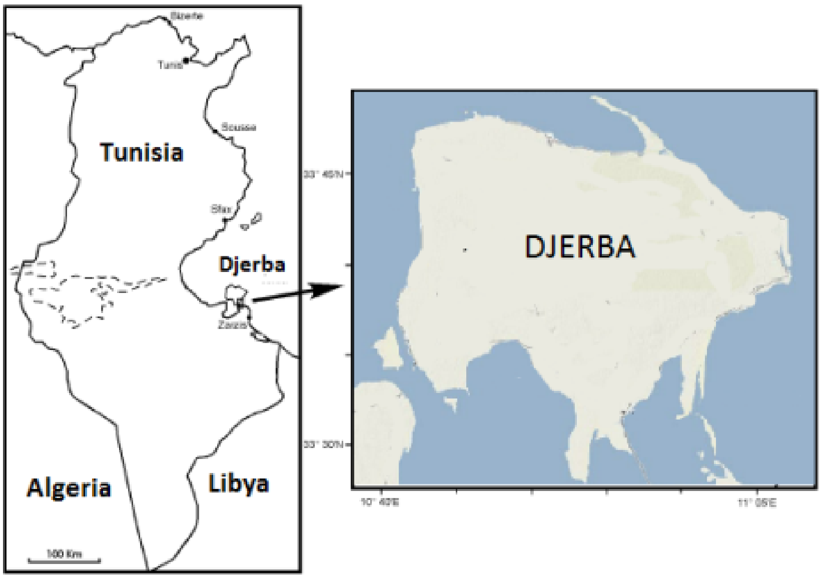

Figure 2.4: Djerba location in Tunisia [13]

2.2.1 Energy mix

The main power source in Djerba is a fossil fuel-based power plant that uses natural gas to produce approximately 140 MW of electricity, which covers roughly 70% of the island's energy needs. The remaining demand is met through electricity that is imported through submarine cables from the mainland. The fossil fuel power plant emits around 63 tons of metric CO^2. [20]

The total electricity consumption on Djerba Island is around 300 GWh annually. Hotels use 70 GWh, while the residential sector consumes 67 GWh [20]. Another major electricity consumer on the island is the water desalination plant. This plant processes seawater, filtering it to produce fresh water to meet the island's demand. It has a daily capacity of producing 50,000 m^3 of water, which can be expanded to 75,000 m^3 using reverse osmosis technology. Due to its size and the energy-intensive nature of desalination, this plant is one of the largest electricity consumers in the country [22]. According to the project report [33] responsible for the water desalination plant, an estimated 4,5 kWh/m^3 of energy conversion would be used which would consequently result in a daily electricity consumption of around 225,000 kWh per day. A total amount of 810.166 tons of metric CO^2 is released per year from the fuel-oil engine [33].

2.2.2 Challenges

Djerba Island faces significant socio-economic, environmental and energy challenges that impact its development and sustainability.

Socio-economically, the island's economy is heavily reliant on tourism, which leads to seasonal employment fluctuations. During off-peak seasons, the lack of consistent work creates financial instability for the local population. Additionally, other economic sectors on the island are also experiencing crises, further worsening the economic challenges faced by the residents. [20]

Environmentally, Djerba is vulnerable to the effects of climate change. The island is experiencing beach erosion and the degradation of its coastline, which threaten its coastal tourism industry. Projections indicate a potential sea level rise of 50 cm by 2050, which could result in the submersion of land and further beach degradation, with losses ranging from 75 to 135 cm per year. [20]

In terms of energy, Djerba faces high costs for energy supply and a shortage of suitable land for building power stations. These challenges complicate efforts to meet the island's energy demands sustainably. To address these issues, Djerba is touching upon innovative solutions, such as floating solar PV systems, which can help overcome land scarcity and promote renewable energy [20].

Tunisia's broader energy strategy includes diversifying the energy mix with renewable sources, aiming to generate 30% of its electricity from renewable sources like solar and wind by 2030. This transition is crucial for reducing Djerba's carbon footprint and enhancing its resilience to global climate change [20].

Chapter 3

Theoretical background

This chapter delves into the theory behind solar energy and energy storage in addition to addressing some important financial aspects. A literature review of solar PV in the European and African context is presented. Most of the theoretical part is based on courses from the master's program such as TEK5350-5390 Solar Energy and TEK5375 Battery technology.

3.1 Solar Energy

In just an hour and half, the sunlight that reaches the Earth's surface is enough to meet the world's total energy consumption for a full year. Solar technologies harness this power using several methods such as PV panels and concentrated solar power. These systems convert solar energy into electricity, which then can be either directly utilized or stored in batteries or other forms of storage for later use. [**?**].

3.1.1 Solar radiation

Solar radiation refers to the energy emitted by the Sun. The amount reaching just outside Earth's atmosphere can be determined by considering the radiant power density of the sun on its surface (5.961 x 10^7 W/m^2), the sun's radius, and the distance between the Earth and the Sun. This results in an average solar irradiance at the edge of the Earth atmosphere of approximately 1366W/m^2, as shown in Figure3.1. [24]

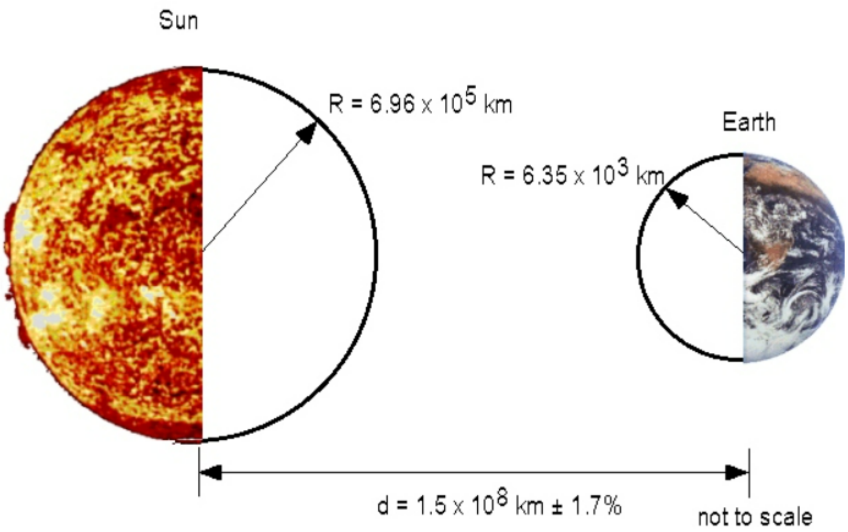

Figure 3.1: Geometrical constants for finding the Earth's solar irradiance[24]

However, the actual power density at any given time is subject to slight variations due to the elliptical nature of Earth's orbit around the Sun and the intermittency of solar power, see Equation 3.1This orbital variance can cause about a 3.4% fluctuation in solar irradiance. [24]

$$\frac{H}{H_{\text{constant}}} = 1 + 0.033 \cos\left(\frac{360(n-2)}{365}\right) \tag{3.1}$$

3.1.2 Atmospheric effects

Solar radiation reaching the Earth's surface is influenced by multiple atmospheric conditions which significantly impact photovoltaic systems. These effects include: [24]

- **Atmospheric Interactions:** Solar radiation is decreased due to absorption, scattering and reflection processes within the atmosphere.
- **Diffuse Radiation:** The atmosphere adds a diffuse or indirect component to the incoming solar radiation, modifying how it is received on the Earth's surface.
- **Local Atmospheric Conditions:** Factors such as water vapor, cloud cover, and pollution can change the power, spectrum, and direction of the solar radiation.

As solar radiation penetrates the atmosphere, it encounters gases, dust and particles that absorb photons. Additionally, the solar radiation is scattered by atmospheric effects. This scattering and absorption affect the overall quality and intensity of solar radiation as it reaches Earth. [24]

3.1.3 Air mass

Air Mass refers to the length of the path that sunlight travels through the atmosphere, standardized to the shortest path length which occurs when the sun is directly overhead. It serves as a measure of how much sunlight is diminished in strength due to absorption by air and dust as it moves through the atmosphere. Air Mass is defined as follows [24]:

$$AM = \frac{1}{\cos \theta_z}$$

Where:

- AM = Air mass
- θ_z is the angle from the vertical also called the zenith angle

In other words air mass is a description of the amount of atmospheric distance the light has travelled and can be expressed as follows:

- AM0: This represents conditions where the light has not passed through any atmosphere
- AM1: This condition occurs when light travles through the atmosphere along a straight path
- AM1.5: Here, light travel through the atmosphere along an inclined path, effectively extending the path length by 1.5 times, corresponding to solar elevation angle of 42°

3.1.4 Irradiation components

Solar irradiation, when interacting with the Earth's atmosphere, can be measured and analyzed in several distinct components. Each component serves a specific purpose and is of interest for various solar energy technologies. The main components of solar irradiation are shown in figure 3.2, and are described below:[36]

Global Horizontal Irradiance (GHI)
GHI measures the total solar energy received per unit area on a horizontal surface. It encompasses both the direct beam from the sun and the diffuse radiation from the sky. This comprehensive measure is crucial for PV power plants as it accounts for the total solar energy available for conversion, both from direct and scattered sources.

Direct Normal Irradiance (DNI)
DNI quantifies the solar energy received per unit area on a surface that is always oriented perpendicular to the sun's rays. This measurement reflects the free sunlight that directly reaches the surface without being scattered in the atmosphere.

Diffuse Horizontal Irradiance (DHI)
DHI represents the solar energy received from all parts of the sky, excluding the sun's direct beam, on a horizontal surface. It results from sunlight scattered by atmospheric elements like aerosols, molecules, and clouds.

Plane of Array (POA) or Global Tilted Irradiance (GTI)
POA/GTI measures the total solar irradiance that strikes a tilted plane, such as a solar PV panel. This includes all direct and indirect solar radiation from the sky, as well as radiation reflected from the ground and surrounding objects.

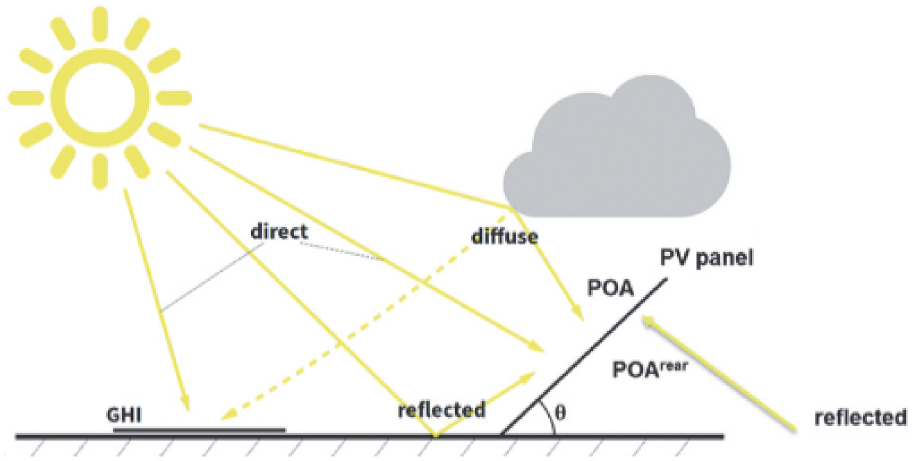

Figure 3.2: Irradiation components and how they shed light on a solar panel β

3.1.5 Standard Test Conditions

Researchers and manufacturers from the solar energy sector use a common reference to evaluate the performance of solar panels. This benchmark is referred as Standard Test Conditions (STC) and it is used to facilitate the calculations and estimations for the solar panels. The STCs include: [24]

- An ambient temperature of 25°C
- Irradiance G = 1000 W/m^2
- Spectral distribution of AM 1.5G

3.1.6 Solar resource data available

Solar resource data is critical for the planning and analysis of solar energy. These data are either measured on the ground or through a satellite. Satellite-derived data can offer a wide geographical coverage and can often be obtained retrospectively for historical periods in which no ground-based measurement were taken. This is especially useful for assessing long term averages.[24]

There exist several data sets available today, to name a few:

Meteonorm
World wide weather data, based on 8325 weather stations and 5 geostationary satellites. Not only for PV – not all the weather stations has irradiation measurements. Default in PVsyst.

Satel-light

The server produces maps for all Europe, data are derived from Meteosat images.

NASA SSE
Archive of over 200 satellite-derived meteorology and solar energy parameters, globally available with high resolution (1x1 deg)

SolarGIS
High resolution solar irradiation database developed from Meteosat MSG data. Available for Europe, North Africa, and Southwest Asia through the SolarGIS web portal.

3.1.7 Solar generation

The power output for the solar PV generation can be expressed in several ways, depending on the user's case. A general approach for calaculating the solar generation of each hour of a year is represented in Equation 3.2: [11], [41], [4]:

$$P_{\mathrm{PV}}(t) = \eta_{\mathrm{mod}} \times A_m \times G_t(t) \times (1 - L) \times N_{\mathrm{mod}} \tag{3.2}$$

where η_{mod} is the efficiency of the PV module, A_m is the area of the panel receiving the solar irradiation (m^2), $G_t(t)$ is the global solar irradiation on a tilted plane with optimum tilt ($\mathrm{W/m}^2$), L are the losses from inverter, charge controller and wires that are included in the PV system, and (N_{mod}) is the number of modules.

The efficiency of the photovoltaic module can be estimated by Eq. 3.3 [10]

$$\eta_{\mathrm{mod}} = \eta_{\mathrm{ref}}\{1 - \beta(T_C - T_{\mathrm{ref}})\} \tag{3.3}$$

with β accounting for the PV module temperature coefficient, T_{ref} as module efficiency and T_C as reference temperature under STC conditions (25 °C). The cell temperature can be calculated by Eq. 3.4 [10]:

$$T_C = T_{\mathrm{amb}}(h) + \frac{(\mathrm{NOCT} - 20) \times G_{\mathrm{t}}(h)}{G_{\mathrm{Nom}}} \tag{3.4}$$

where T_{amb} is the ambient temperature, G_t(h) is the global solar irradiation for each hour, and NOCT is the operating temperature of the PV cell under standard test conditions. The reference efficeicnecy, temperature coefficient, NOCT, and efficiency of the module is data that can be obatined from the PV module manufacturers, and it differs from one manufcaturer to the other, depending on the size and power output of one module.

3.2 Battery storage

Batteries that are included in a solar energy system, plays a central role of the overall system which significantly affect the cost, maintenance requirements, reliability and design of the PV system. Because of this large impact that batteries have on a stand-alone solar system, it is important to understand the properties behind the battery. In a ideal situation, or in a perfect world, the battery used in such a system would be able to be charged and discharged indefinitely under arbitrary charging/discharging regimes, would have high efficiency, high energy density, low-self discharge and be low cost. However, these parameters are affected by the battery type and its usage in the system. In practice, no battery can achieve such requirements and is therefore crucial to understand the key metrics of a battery.[25]

3.2.1 Key metrics

- Voltage [V]: Refers to the potential electrical energy in a circuit. It is the voltage that generate electrical current
- Current [A]: Refers to the electrical current, the flow of the electrical energy
- Power [W]: Is the product of voltage and current
- C-rate: It is a measure of charging and discharging rate of the battery. 1C means charging a battery from 0-100% in one hour.
- State of charge (SOC) [%]: 100% is when the battery fully charged and 0% is when the battery is fully discharged. Commonly, the battery's SOC is limit to avoid fully charged or discharged state. (80% max charge, 30-40% max discharge). Therefore, the effective SOC range refers to the actual possible SOC range after restriction
- Cycle: One cycle is discharging the battery from 100% to 0% and charging it to 100% again. If the battery doesn't fully discharge or charge, then it is referred to as a "partial cycle". [6]

3.2.2 Battery efficiency

One of the most important attributes of battery energy storage systems is its efficiency. The efficiency of a battery is the ratio between the energy output and input of the battery. Different batteries have different efficiencies dependent on their applications, chemistry and battery setup. [6]

The efficiency of a battery is specified by two efficiencies:

- Columbic efficiency: is the ratio between the number of charges that enter the battery compared to the number that can be extracted from the battery during discharging (typically at 95%)
- Voltage efficiency is influenced by the difference between the charging voltage and the discharging voltage of a battery, which is also influencde by how the battery voltage varies with its State of Charge.

Energy, Volumentric, Power density
Energy density measures a battery's capacity relative to its weight or volume, expressed in Wh/kg (gravimetric) or Wh/dm3 (volumetric). A higher energy

density means a lighter battery for the same capacity. While crucial in portable systems, energy density is less critical in stationary photovoltaic (PV) systems, although high energy density can reduce transportation costs to remote locations. Power density, which considers both energy density and discharge speed, is important in transport applications but generally not in PV systems. [25]

3.2.3 Capacity

Capacity: The capacity of the battery is the maximum possible energy discharged from the battery. It can be given in either Ah, representing the charge capacity, or Wh, representing the energy capacity. There isn't any standardization of the different terms for capacity, but here is an attempt to summarize the most common ways to refer to the capacity of the battery. nominal capacity, rated capacity, installed capacity, maximum capacity, or maximum effect is how many Ah or Wh the battery can provide under specific conditions and is usually provided by the manufacturer at the beginning of life. The usable, effective, or actual capacity is the capacity that the battery is actually able to deliver. [6] DOBBELCHECK THIS, and what more needs to be done?

3.2.4 Comparison of battery characteristics

Table 3.1 serves as a comparison between the different batteries and highlights its specifications and characteristics. [6][26]

Table 3.1: Comparison of Battery Characteristics

Battery Chemistry	**Application**	**Specific Energy (Wh/kg)**	**Cycle Life**	**Cost ($/kWh)**
Lead Acid	Automotives, renewable energy storage	30-50	300-500	$150-200
NiCd (Nickel-Cadmium)	Portable electronics, aviation, backup power	40-60	2000-3000	-
NiMH (Nickel-Metal Hydride)	Consumer electronics, hybrid vehicles	60-120	500-1000	$500
Li-ion (Cobalt)	Mobile phones, laptops	150-190	500-1000	$300-500
Li-ion (Manganese)	EVs, power tools	100-150	1000-2000	$250-400
Li-ion (Phosphate)	EVs, large-scale energy storage	90-120	2000-3000	$250-350
Vanadium Redox Flow	Utility-scale storage	20-35	>1000	-

3.2.5 Battery equations

To ensure the reliability of the battery with respect to its lifetime, degradation and electricity supply, these equations describes conditions so that the battery operates in a safe way. The battery capacity during discharge and charge can be expressed below. Equation 3.5. represents the battery's SOC during charging at hour t [10] [44][8].

$$SOC(t) = SOC(t-1)(1-\sigma) + \left[P_{\mathrm{PV}}(t) - \frac{E_L(t)}{\eta_{\mathrm{inv}}}\right] \cdot \eta_{\mathrm{bat}} \tag{3.5}$$

Equation 3.6 represents the SOC during discharging at hour t

$$SOC(t) = SOC(t-1)(1-\sigma) + \left(\frac{E_L(t)}{\eta_{\mathrm{inv}}} - P_{\mathrm{PV}}(t)\right) \cdot \eta_{\mathrm{bat}} \tag{3.6}$$

where $SOC(t)$ and $SOC(t-1)$ represent the electricity stored in the battery for hours t and t-1, σ is the self-discharging factor (normally 3% [9]), η_{bat} and $\eta_{\mathbf{inv}}$ is the efficiency of the battery bank and of the inverter, respectively.

To preserve the efficiency and the operations standards of the battery the value of $SOC(t)$ must be preserved in a way so it does exceed the minimum permissible energy level SOC_{min}, which ensures the battery bank maintains a minimum charge. Furthermore, during the charging operation, the value of $SOC(t)$ must not exceed the maximum allowed energy level SOC_{max}. Eq 3.7 shows these constraints. [37]

$$SOC_{\mathrm{min}} \leq SOC(t) \leq SOC_{\mathrm{max}} \tag{3.7}$$

The maximum state of charge, SOC_{max}, equals the nominal capacity of the battery bank, C_{Batt}. The minimum state of charge, SOC_{min}, depends on the battery bank's depth of discharge, DOD, and can be expressed as:

$$SOC_{\mathrm{min}} = (1 - DOD) \cdot C_{\mathrm{Batt}} \tag{3.8}$$

3.3 Financial metrics

To conduct an economic analysis of an energy system, several financial metrics must be addressed in order to evaluate the viability of the system. Levelized cost of energy (LCOE), is a metric that is commonly used to compare the cost of energy from different generation technologies. It is expressed in cost per unit of energy generated ($ per kWh), and is represents the installing and operating costs of an energy system over an assumed financial life and duty cycle, see Equation 3.9 [3], [45], [15].

$$\mathrm{LCOE} = \frac{\mathrm{NPC} \times \mathrm{CRF}(d,l)}{\sum_{i=1}^{l} E_{\mathrm{gen}}(t)} \tag{3.9}$$

where NPC is the net present cost ($), $\mathrm{CRF}(d,l)$ represents the capital recovery factor, d is the discount rate (%), l is the project lifetime and $E_{\mathrm{gen}}(t)$ is the energy generated at hour (t).

Another economic metric that is valuable to assess the cost-effectiveness of a system is the NPC. It represents the total cost of a system over its lifetime, discounted to the present-day values. It includes all, capital, maintenance, operational, and replacement costs, minus any revenues generated by the system, see Equation 3.10. [15],

$$\text{NPC} = \frac{A_{\text{tot}}}{\text{CRF}(d, l)} \tag{3.10}$$

where A_{tot} is the total annualised costs ($/year), d is the discount rate (%), l is the project lifetime, CRF is the Capital Recovery Factor. The discount rate normally ranges between 10-12% according to IRENA [35], and a conservative 10% discount rate was used in this study.

Equation 3.11 represents the Capital Recovery Factor (CRF) which is a factor used to calculate the annuity payment needed to cover the capital cost of an investment over its lifetime. It translates the total initial investment into a series of equal annual payments, considering the time value of money.[42]

$$\text{CRF}(d, l) = \frac{d(1+d)^n}{(1+d)^n - 1} \tag{3.11}$$

where d is the discount rate (%) and n is the number of periods (years).

3.4 Literature review

3.4.1 PV uptake in North Africa

Being Africa's largest energy market, North Africa has an energy landscape that differs from the Sub-Saharan countries. Oil and natural gas are the primary energy sources in these countries in contrary to biomass in the rest of the continent. Gas-fired power plants in the region, that supplies electricity, stand for 82% of the total power plants in the continent which reflect the size of the energy market [35].

Unlike the rest of the continent, Northern African countries have almost universal access (99%) to electricity, with the exception of Sudan. This high rate of access is tied to the region's extensive use of natural gas and oil for electricity generation and significant investment in power generation and transmission. [34]

According to IRENA [35], North Africa possesses the continent's greatest potential for solar energy development due to its high annual average solar irradiation accounting of 2200 kWh/m^2. The installed solar capacity, including both PV and thermal, has increased significantly over the past five years, reaching more than 3,000 MW in 2020. However, this capacity still represents just 2.7% of the region's total installed electricity generation capacity of approximately 116 GW. There are regional differences, with the share of solar installed capacity ranging from less than 0.1% in Libya to over 15% in Mauritania. [34]

Egypt and Algeria have been pivotal in the installation of solar PV power plants, collectively accounting for 84% of the total solar PV installed capacity in North Africa in 2020. Most of this solar power capacity is grid-connected, while off-grid capacity is primarily found in Algeria's isolated southern areas. Concentrated solar power (CSP) is also significant in the region, with Morocco holding over 90% of the CSP capacity in 2020, mainly due to the 510 MW Noor-Ouarzazate plant, the world's largest CSP plant. Algeria and Egypt have smaller CSP plants, each with a capacity of 20 MW, inaugurated in 2011. The Algerian government aims to reach 2 GW of CSP capacity by 2030 [34]

The average total installed cost for solar PV in North Africa decreased from USD 2000/kW in 2015 to USD 1306/kW in 2019. This data includes 38 projects in North Africa. Globally, the installation cost for solar PV fell from USD 1800/kW to USD 995/kW during the same period. Recent projects in Tunisia for independent power producers averaged USD 30/MWh, with the lowest bid for a 200 MW solar plant in Tataouine at approximately USD 24/MWh, the lowest solar bid recorded in Africa at that time. Despite declining cost trends, solar CSP plants remain more expensive than solar PV plants, with the NOOR III CSP plant having a total installed cost of USD 5367/kW [34].

An overview of the cost range for solar energy in different segments is presented in Table 3.2, which varies between system configurations mainly due to the size of the solar powered system.

Table 3.2: Solar PV Costs in Africa

Segment	**Cost Range (USD/W)**
Utility-scale solar PV	1.35 - 4.1
Grid-connected mini-grids (without batteries)	2.5 - 3
Off-grid mini-grids (without batteries)	1.4
Mini-grids (with battery storage)	2.4 - 5.9
Solar home systems ($<$ 1 kW)	4 - 16
Solar home systems ($>$ 1 kW)	3.6 - 17

3.4.2 RES powered water desalination plant

A water desalination plant is the process of converting seawater or brackish water to fresh water. According to the International Desalination Association (IDA), there are currently about 20,000 water desalination plants in the world, producing 109 million m^3/day fresh water to over 300 million people [27]. Several water desalination technologies exist, with reverse osmosis technology (RO) accounting for 65% of the total plants worldwide. Solar PV can serve as an ideal technology for powering RO units especially in rural areas where no grid connection is available [1]. Combining solar PV and water desalination plant can be setup as a standalone or as a hybrid energy system, with one or more energy storage/conversion sources such as batteries, wind, hydro, fossil fuel generator and grid connected.

Several studies highlight the combination of water desalination plant with hybrid energy system and standalone solar PV generated. Tzen et al. (2007) [52] conducted a study in Greece on a real system in operation where a solar and wind powered energy system was connected to a RO unit for seawater desalination. The system consisted of 3.96 kWp PV panels, a 900 Wp wind turbine, a battery bank of 44.4 kWh and two inverters. The overall production was measured at 3.12 m^3/day of fresh water and an energy consumption of 16.5 kWh/m^3. The overall energy consumption was reduced by about 50% compared to conventional grid-powered systems which demonstrates the feasibility of a hybrid renewable energy system for a RO unit. They highlighted important metrics that are important for future RES integrated systems, such as design, and energy and material selection.

The deployment of a 2 kWp solar PV system paired with a battery bank to power a 600 W RO unit in Malaysia was analyzed by Alghoul et al. (2016) [5] in their study. The research focused on the performance of the battery under varying climatic performances, assessing its power output both during the day and at night. The results showed that the battery could sustain operation for 11 hours during the day and 11.5 hours at night. However, it was observed a 50% reduction in the battery performance mainly due to high temperatures reaching 45°C in the battery room. These findings highlight the critical need for thermal regulation within battery storage areas to maintain optimal battery efficiency and performance.

In a feasibility study conducted in Iran, by Rahimi et al. (2021) [48], various scenarios integrating solar PV with small-scale RO desalination systems were analyzed to address water shortages. The study evaluated the economic impact of different configurations combining solar and grid electricity, including scenarios where excess solar electricity is sold back to the grid. The findings showed that systems allowing for electricity export during peak solar hours offered the highest net present value (NPV), displaying the potential for economic viability in solar-powered desalination. On the other hand, scenarios reliant on battery storage demonstrated negative NPVs, highlighting the economic challenges posed by storage costs and low local electricity prices.

Fthenakis et al. (2016) [23] demonstrate the economic benefits of using solar photovoltaic (PV) systems for RO desalination in high solar irradiance areas like Saudi Arabia. Their analysis show that PV systems, particularly with one-axis tracking, can achieve electricity costs as low as $0.09/kWh, substantially reducing costs of diesel-powered systems. Large-scale solar RO plants could displace up to 33.5 million liters of diesel per year, saving $43.2 million in subsidies and reducing CO^2 emissions by up to 90,241 tonnes annually. This highlights the potential of solar-powered desalination as both an economically and environmentally viable solution for arid regions. [23]

Kumarasamy et al. (2015) [38] explore the efficient operation of small solar-powered RO desalination plants, particularly those that operate without battery storage in areas with unreliable grid power. The study assessed two strategies: operating without any permeate storage and using a buffer tank for permeate storage. The findings indicate that avoiding batteries reduces both capital and maintenance costs, while incorporating a buffer tank can increase permeate production by 28% to 36%, serving as a new format of energy storage. The research demonstrates that with good management of solar power and permeate storage, these RO plants can increase the overall performance and handle solar viability effectively, providing a sustainable and cost-effective solution.

3.4.3 Modeling a solar PV system

Modeling a solar PV system with storage is a complex matter where the parameters used need to be considered carefully. To find the right modeling set up and techniques as well as the required input and desired output parameters for the feasibility of a stand alone energy system in Djerba, necessary research was done.

Studies differ from one another in terms of input parameters, simulation tools, energy system set up and the study area. Agua et.al (2020) [2] conducted a comparative analysis of decentralized and clustered microgrid systems on the Polillo island groups, Philippines, using HOMER Pro and GIS modeling. The study evaluated solar PV, Li-ion battery storage system and diesel generator, aiming at optimizing the LCOE while enhancing system reliability. Inputs such as solar irradiance, existing diesel capacities and demand profiles of each island were integrated in the simulations. The optimal component configurations (size and capacity) and LCOE assessment under various scenarios were the outputs of this research.

Bakelli et.al (2011) [11]dexplores the development of a sizing model for PV water pumping systems in Algeria. Utilizing a comprehensive modeling approach that incorporates the loss of power supply probability (LPSP) for assessing system reliability and the life cycle cost (LCC) for economic evaluation, the study optimizes the configuration of photovoltaic arrays and water storage capacities. The model inputs include solar irradiation, ambient temperature, and water consumption profiles, leading to outputs that define optimal system configurations alongside economic and reliability metrics. This approach is particularly suited for remote, arid regions where reliable and cost-effective water supply systems are critical, demonstrating significant potential for enhancing both the reliability and economic efficiency of photovoltaic water pumping systems.

Ajiwiguna et.al (2021) [4] investigates the integration of a PV system with RO desalination, augmented by a seasonal water storage tank (SWST),to stabilize water supply without using batteries. Conducted on Wando Island, South Korea, the research uses scientific Python algorithms to optimize the sizes of the PV array, RO unit, and SWST based on local solar irradiation and ambient temperature data. This optimization aims to minimize water production costs, achieving rates as low as \$1.74/m^3 for constant demand scenarios and \$2.59/m^3 for variable demand scenarios. By excluding traditional battery storage, the study addresses cost and lifespan issues associated with batteries, presenting a viable alternative that leverages excess water storage during peak production periods to ensure a steady water supply despite fluctuating solar power availability.

Farhani et.al (2024) [21] evaluates a hybrid system designed for an agricultural farm in Kairouan, Tunisia, utilizing HOMER Pro software. The hybrid system evaluated includes PV panels and a hydrogen fuel cell alongside a water desalination unit, optimizing for efficiency and cost-effectiveness based on local solar irradiation and demand profiles. Inputs such as solar data, component specifications, and demand requirements guide the model to determine optimal configurations for PV arrays, electrolyzers, hydrogen storage, and fuel cells, with outputs including system configuration, LCOE and reliability assessments. The findings affirm the system's potential to reliably meet agricultural energy and water needs, reduce dependency on conventional energy grids, and cut operational costs, underscoring the feasibility of solar hydrogen systems in arid regions like Tunisia.

Suresh et.al (2020) [49] analyzes a multi-source hybrid energy system designed to power three rural villages in Karnataka, India. Utilizing both Genetic Algorithm (GA) and HOMER Pro software for optimization, the system integrates solar, wind, biomass, and biogas energy sources alongside a fuel cell and battery storage to maximize reliability and cost-effectiveness. The modeling focuses on minimizing the Total Net Present Cost (TNPC) and Cost of Energy (COE), while also aiming to reduce CO^2 emissions and the unmet load. The results demonstrate that the GA-based model outperforms those configured with only HOMER Pro, suggesting that such a hybrid system can significantly enhance the sustainability and economic feasibility of rural electrification in challenging environments. [49]

Trapani et.al (2024) [51] evaluates the integration of renewable energy sources with hydrogen and battery storage to electrify remote Norwegian islands. The study employs a techno-economic optimization framework to determine optimal system configurations that minimize the LCOE while ensuring a reliable 100% renewable power supply. The analysis focuses on the technical and economic feasibility of replacing diesel generators and avoiding extensive transmission infrastructure through localized RES setups enhanced with hybrid storage solutions. Key findings highlight the critical role of hydrogen storage in reducing the need for large battery and RES capacities, demonstrating lower LCOE and better environmental outcomes compared to conventional diesel-based systems. This study offers valuable insights into designing and implementing cost-effective and sustainable energy solutions for isolated communities.

Ouedering et. al (2022) [44] focuses on developing a sustainable power solution for Djerba, Tunisia, integrating PV panels, wind turbines, tidal turbines, battery storage and a diesel generator. Utilizing HOMER software and MATLAB for simulation, the research aims to optimize the configuration to minimize life cycle cost (LCC), embodied energy (EE), and maintain a zero probability of loss of power supply (LPSP). This hybrid system is evaluated for its ability to meet the energy demands of the island efficiently, highlighting the cost-effectiveness and environmental benefits over traditional power sources. The findings demonstrate that such a system can significantly enhance reliability and reduce operational costs, offering a viable model for energy sustainability in remote locations.

3.4.4 Modeling tools

Several modeling tools and software exist today to enhance the feasibility of an optimization model. The utilization of the tools depend on the user's needs and objective with the research in case. The tools used in this paper are described below. In addition to these, there exist other tools such as Pyomo (Python Optimization Modeling Objects) library from Python software, HRES, MATLAB and Simulink that are widely known in the academic and scientific community.

GAMS
The General Algebraic Modeling System (GAMS), developed by the World Bank in the 1970s and further refined by GAMS Development Corporation, is a high-level mathematical optimization modeling system. It facilitates the formulation and solution of large-scale optimization problems, including linear, nonlinear, and mixed-integer programming. Widely used in sectors like energy, economics, and supply chain management, GAMS provides flexible and efficient modeling of complex systems. With a full set of solvers and optimization tools, GAMS identifies optimal solutions based on cost-effectiveness, resource utilization, and technical and economic constraints, aiding decision-making across various industries. [18]

HOMER
Hybrid Optimization Model for Electric Renewable, developed by the U.S. National Renewable Energy Laboratory (NREL) in 1993, is a comprehensive software designed to assist in the design and comparison of hybrid energy systems. It simulates the physical behavior and life-cycle cost of power systems while allowing users to compare different design options based on technical and economic parameters. With a wide range of components, including wind turbines, PV panels, diesel generators, batteries, and fuel cells, HOMER calculates the net present cost, renewable electricity fraction, emissions, and fuel consumption of both off-grid and grid-connected hybrid power systems, providing insights into the most cost-effective configurations based on load profiles, renewable energy potential, and component specifications. [39]

3.4.5 Summary of literature

In summary, although the contribution of solar energy to North Africa's electricity mix remains relatively small, its importance has grown significantly. The economic and environmental competitiveness of solar energy makes it a highly viable alternative to fossil fuels in the short and medium term. North Africa's solar energy sector has shown promising growth, and continued investment and development could further enhance its role in the region's energy landscape [34] Despite the incentives that have showed a decrease in the solar power production per kWh, and solar energy being emerged as one of the most promising renewable energy sources in the most of the countries, these achievements are not reflected on the African continent.

The challenges with having reliant grid-infrastructure, lack of investments and reliable investors, the same enhancement in solar energy on the continent has not seen anything similar. Despite having great solar and wind resources, the renewable energy sources have not been uplifted yet.

However, many countries have shown dedication and having aligned with the commitment to reduce global GHG emissions through national plans that aim at integrating more renewable energy resources and decrease the fossil-fuel based power plant reliance.

Microgrid and offgrid renewable based renewable energy systems have shown good promises in terms of costs and energy reliability which could help the African rural regions getting access to electricity. Table 3.3 shows the main technical and economic parameters that are used based on both offgrid and hybrid renewable energy systems. This will help the study get a good overview over which input and outputs parameters are to use to integrate solar PV with battery storage on Djerba Island.

Table 3.3: Technical and economic parameters from papers

System Components	Technical - per source	Economic - Whole system	Ref.
PV	GHI and efficiency	LCOE, NPC, Discount rate	
Li-ion battery	RT efficiency, C-rate, DOD	CAPEX & OPEX, lifetime	[1]
Diesel	Capacity	fuel price and submarine cable cost	
PV	Efficiency, area, ambient temperature, GHI, nr of panels	LPSP, LCC, lifetime, unit price	
Pumping subsystems	Water flow rates and consumption profile	CAPEX & OPEX, interest rate	[11]
Water storage tank	Tank capacity and SOC	NPC, inflation rate	
PV	Module specifications, TMY data, NOCT, tilt and azimuth	Lifetime OPEX & CAPEX	
SWST	Water demand data and storage capacity	Water cost, land cost	[4]
PV	GHI, ambient temperature, efficiency	LCOE, CAPEX & OPEX	
Hydrogen (fuel cell)	Efficiency, capacity, ambient temperature	NPC	[21]
PV	GHI, efficiency, capacity	Total net present cost (TNPC)	
Wind	Wind speed, power curves, efficiency	Cost of energy (COE)	
Biomass/biogas	Availability	OPEX & CAPEX	[49]
Hydrogen (fuel cell)	Efficiency, capacity	Fuel costs	
Battery	Capacity, C-rate, efficiency	Payback Period	
PV	GHI, wind speed, temperature	LCOE, NPC	
Hydrogen (fuel cell)	Storage capacity, efficiency, energy density	CAPEX & OPEX	[51]
Battery	Capacity, efficiency, SOC, lifecycle	Discount Rate and Payback Period	
PV	GHI, solar panel characteristics	LCOE, CAPEX & OPEX, water cost	[38]
PV	Efficiency, array area, GHI	LCC, CAPEX & Opex	
Wind	Capacity, air density, wind speed	LPSP, Discount rate	
Tidal	Capacity, flow speed	Cost of Energy	[44]
Battery	Storage capacity, SOC, C-rate	Embodied energy	
Diesel	Capacity, fuel consumption, efficiency	Inflation rate	

Chapter 4

Data collection and pre-processing

To create an optimization model, reliant input dataset is key to assess the objective of the simulation. This chapter describes the methodology of obtaining and processing necessary data that are used later in the optimization model.

4.1 Solar resource assessment

There are many tools that facilitate the assessment of solar resources in Djerba. For the sake of this study, PVGIS software was used to obtain hourly data throughout a year. TMY, typical meteorically year, is a dataset composed of hourly meteorological values for a specific location, synthesized from data collected over an extended period, typically for a ten year period [16]. The TMY downloaded for this study represented a typical year from the years 2005-2020. The TMY dataset provides an hourly resolution for different parameters, such as GHI, DHI, DNI, air temperature, wind speed etc, where only GHI, DHI, DNI and air temperature are to be considered in this study. Figure 4.1 illustrates the values of the different irradiation components throughout a year in Djerba expressed in W/m^2. In a typical year there are approximately 3741 of sunny hours (more than 100 W/m^2), and the total of:

- GHI is 2097.5 kW/m^2
- DNI is 2379.1 kW/m^2
- DHI is 635.9 kW/m^2

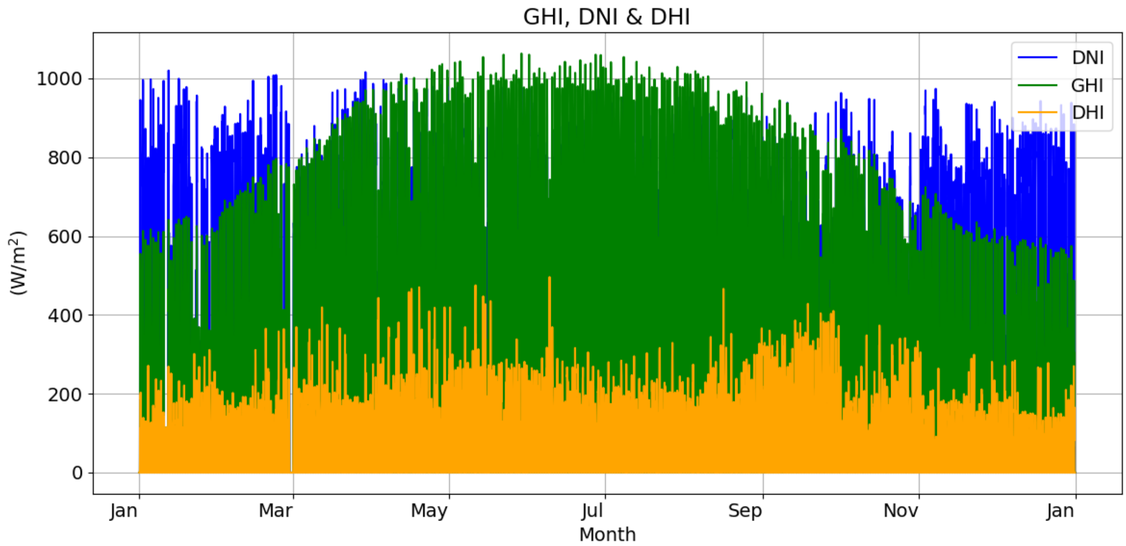

Figure 4.1: Solar irradiation for a year from PVGIS

The air temperature, or the ambient temperature, is shown in Figure 4.2. The average temperature in Djerba is measured at about 22 °C with temperatures exceeding 35°C from May to October , reaching a temperature high of of 41.4 °C in the beginning of September and a temperature low of 7.8 °C in January.

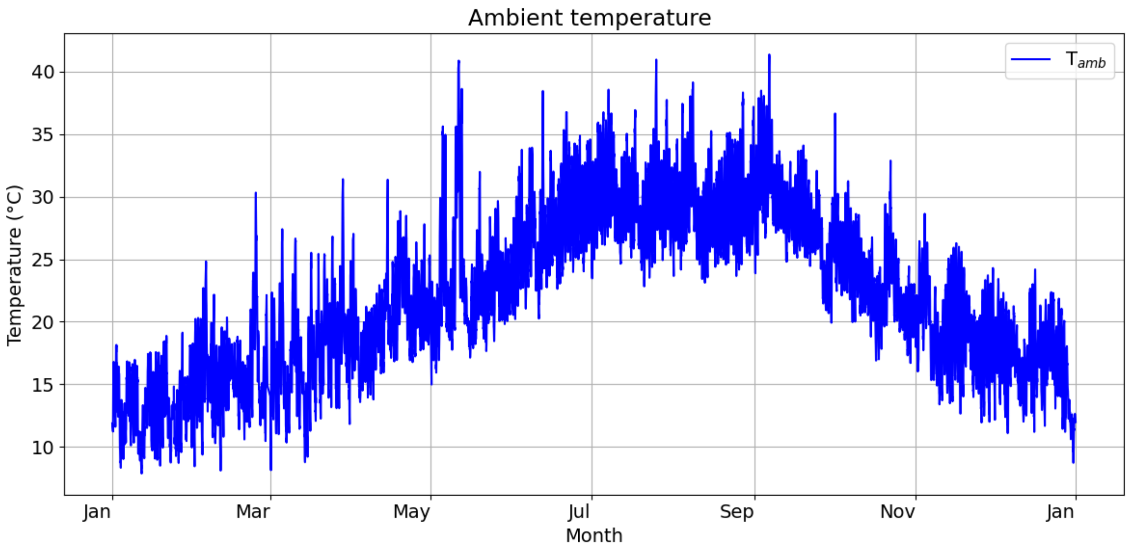

Figure 4.2: Ambient temperature from PVGIS

To estimate the proper solar power generation by one module, the irradiation and ambient temperature datasets are included in the calculations. This is shown in 6.1.2.

4.2 Electricity demand

As explained in chapter 2.2.1 the total electricity consumption on the island for a year was 300GWh. To estimate the solar energy production for a year, accurate hourly resolution data for a year is needed. However, this proved to be more challenging than expected. Unlike open source platforms such as ENTSOE-E and Renewable Ninja, that provide accurate and reliable hourly data for European and other well-developed countries, data on electricity demand in Tunisia is not publicly available. Despite reaching out to various sources, including government departments and companies like STEG, ANME, and Aqualia no responses were received. However, SONEDE, the state-owned enterprise responsible for managing, constructing, and maintaining the country's water supply, did provide some useful data, as shown in **Appendix A**. These data only represent the electricity consumption for the water desalination plant in Djerba, as SONEDE was one of the companies responsible for developing it.

4.2.1 Water desalination plant

To fabricate a synthetic profile that accurately represents the electricity consumption of the water desalination plant throughout the year, it is necessary to accumulate the water consumption of the island. However, due to challenges occurring about finding data, a simulated water consumption data was generated, see Chapter 4.2.1.

The water consumption profile was then adjusted to match the total electricity consumption of 43.1GWh from 2023. Table 4.1 presents the total monthly and annually electricity consumption from the water desalination plant and the total annually electricity costs in \$ (1 TND = 0.32 USD as of 2023), which roughly translates to 0.11 \$/kWh.

To convert the water production into electricity consumption, a conversion rate of 4,5kWh/m^3 was used, as indicated from the project planning of the RO-unit [33]. Figure 4.3 represents the total electricity consumption of the RO-unit during 2023 with variations from the estimated water consumption. Seasonal water demand is indeed affecting the electricity consumption as show in Figure 4.4, which illustrates a summer and winter daily profile with an average daily consumption of 118.6 MWh.

Table 4.1: Monthly and yearly total electricity consumption of the desalination plant in GWh (2023) A

Month	**Total**
January	2.9
February	2.2
March	3.0
April	3.8
May	3.5
June	3.6
July	4.5
August	4.4
September	4.1
October	4.2
November	3.8
December	3.1
Total annually (GWh)	43.3
Total annually (US$)	4.8M

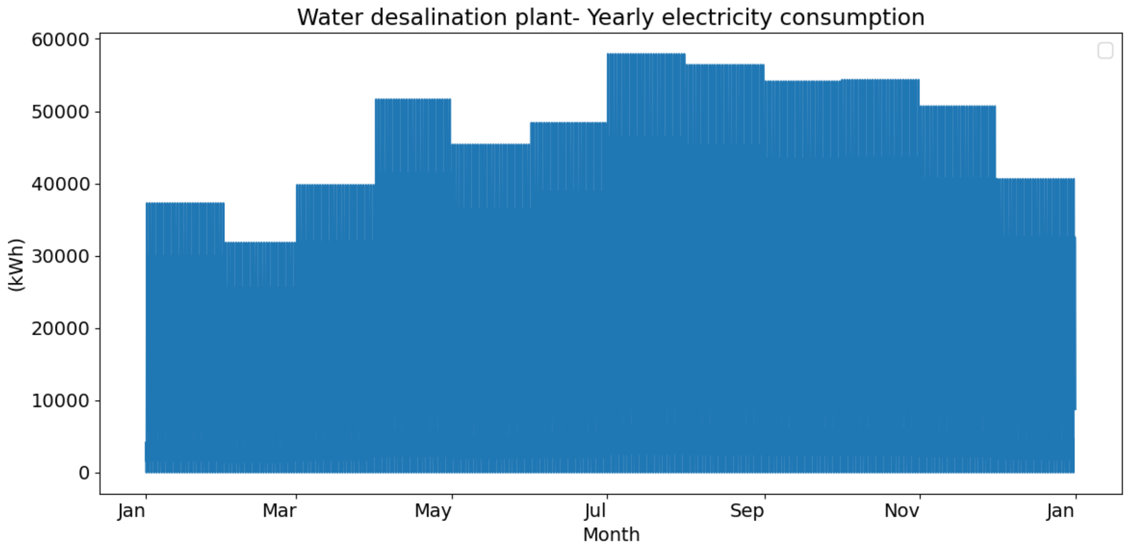

Figure 4.3: Yearly electricity consumption of the water desalination plant

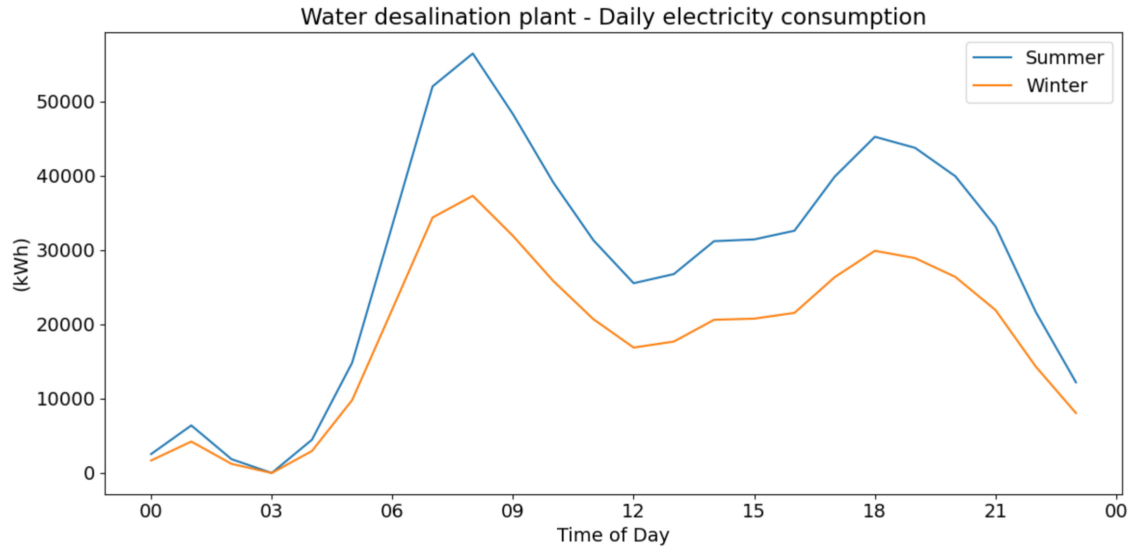

Figure 4.4: Summer and winter daily electricity consumption profiles

Water consumption

Water consumption generally varies throughout a day, typically peaking in the morning and evening hours of the day. Figure 4.5 shows a typical daily water consumption profile, representing the hours from 0 to 24. The data for simulating this pattern is derived from a sine function, as shown in the Eq. 4.1 [38]:

$$Q_d(t) = \sum_{i=1}^{6} a_i \sin(b_i t) \tag{4.1}$$

where $Q_d(t)$ and t are rate of consumption in m^3/h of the day in hours. The values of ai, bi, ci are given in Table 4.2

Table 4.2: Values of parameters for water consumption model [38]

Constants	**1**	**2**	**3**	**4**	**5**	**6**
a_i	0.04689	0.01211	0.00828	0.00446	0.00307	0.00106
b_i	0.13250	0.25520	0.52360	0.78640	1.04700	1.83200
c_i	-0.03340	1.84590	-2.75700	1.52500	0.25410	0.74880

Based on the total electricity consumption from the water desalination plant, the generated water consumption profile, and the conversion rate of 4,5kWh/m^3 a total of 9,624,286 m^3 was produced in 2023 with a daily average of about 26,368 m^3.

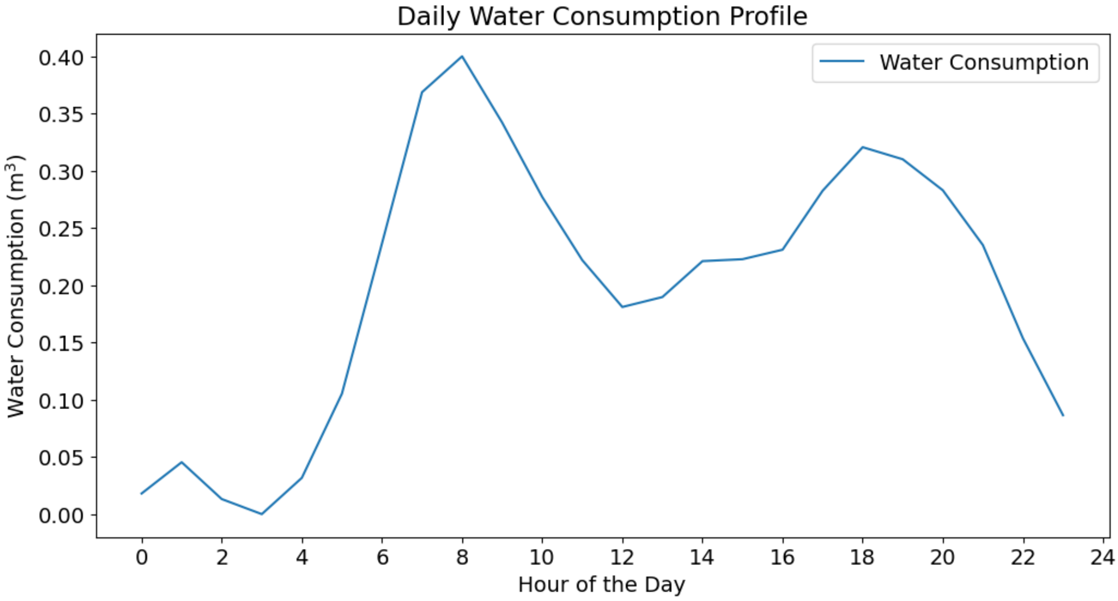

Figure 4.5: Daily water consumption profile

4.2.2 Residential sector

To simulate accurate hourly resolution data, a synthetic electricity consumption profile was generated with HOMER Pro software which uses satellite based data and provides hourly data throughout a year driven by the user's requirements. The baseload, which is the consistently required electricity demand driven by essential appliances and equipment, is included [39].

The hourly data accumulated was generated with a default value at 11.35 kWh/day. [46]. Since the total electricity consumption in the residential sector was 67 GWh in a year, as mentioned in Section 2.2.1, some adjustments are needed. Applying a scaling factor of 1.8, a more accurate set of synthetic data was then generated. The scaling factor is based on the ratio between the total electricity consumption in a year and the total electricity consumption from the generated data from HOMER Pro. The "new" generated profile is shown in Figure 4.6 which illustrates the daily electricity consumption in summer and winter, and highlights a peak demand of 34,000 kW occurring at 6 p.m in summertime. The revised profile indicates an average daily electricity consumption of the whole residential sector at 184 MWh.

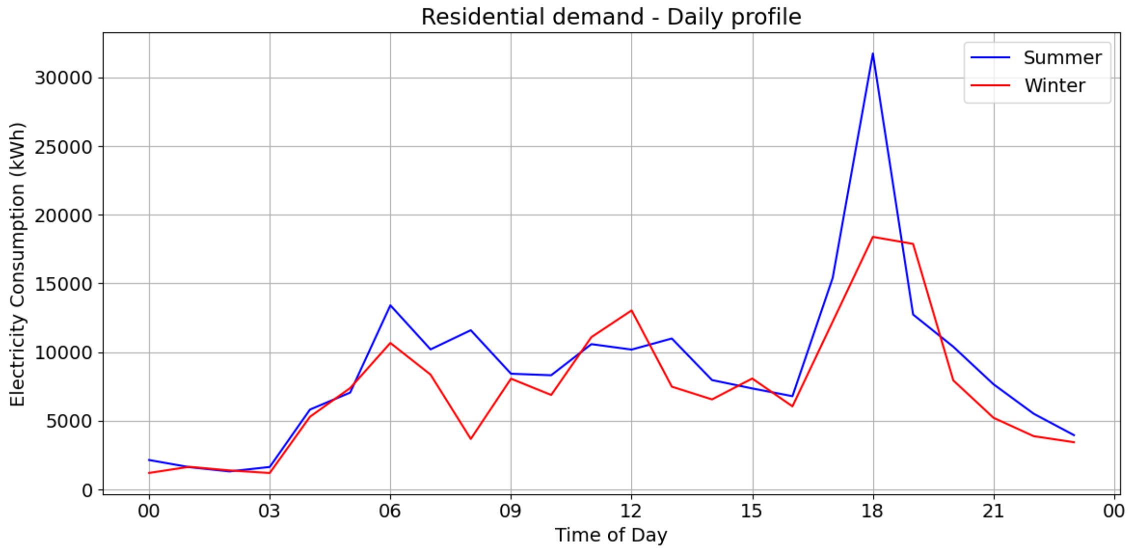

Figure 4.6: Electric load profile in the residential sector

4.2.3 Hotel sector

Assessing the electricity consumption from all the hotels in Djerba, proved to be challenging as well. These are not easily accessible to the public. Several hotels, differentiating mainly in size, were contacted and asked for hourly data of the electricity consumption, but with no response. Therefore, generating synthetic data for the hotel industry is a reasonable solution.

HOMER Pro software generated synthetic data of the residential sector, as explained earlier, and provided hourly data for both the commercial and industrial sectors. The hotel sector would typically "fall" under the commercial sector in this case, but after detailed analysis of dataset representing the commercial sector, this was excluded in this study. It seemed not reasonable to not include this as an illustration plot from this dataset, showed that the electricity consumption was high from 6-7 o'clock in the morning till 18 o'clock in the evening, and was close to zero in the other hours of the day. This indicates that the commercial sector from HOMER Pro, includes mainly service building and bureaus, where come to work in the morning and leave in the evening, typically at 18 o'clock in Tunisia.

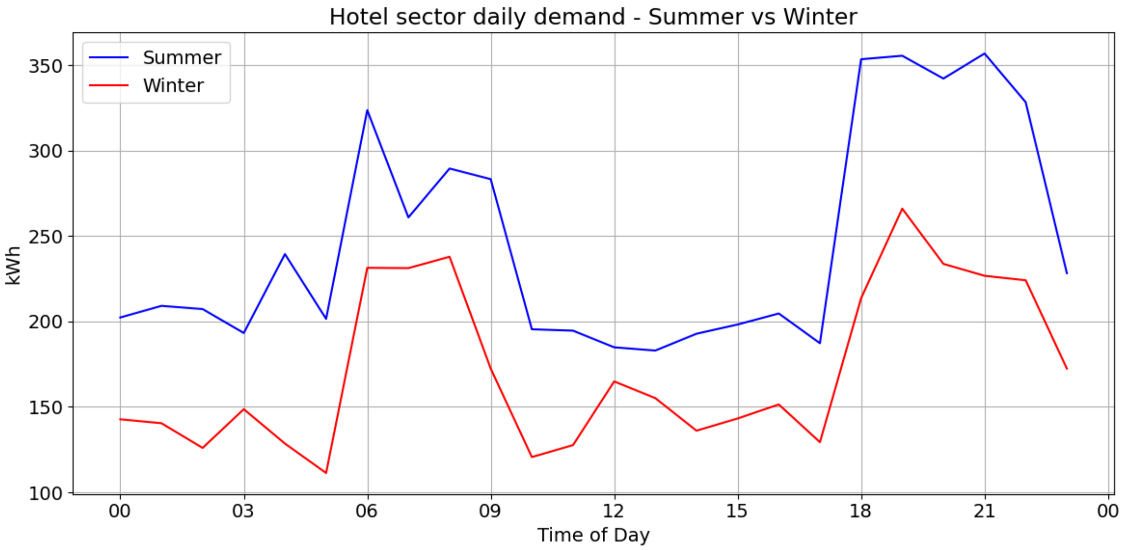

Figure 4.7: Electric load daily profile for the hotel sector

A new synthetic dataset was generated based on typical hotel behaviour throughout a year for Mediterranean located regions. This synthetic hourly dataset is based on higher electricity demand between April and September and lower in the off-season. These values are then readjusted to the estimated total electricity consumption from hotels mentioned in 2.2.1, with a total of 70 GWh. With a scaling factor of 38.3 the new synthetic dataset is illustrated in Figure **??** which represents the daily profile between summer and winter. Peak demand of 16071 kWh occurs in July with an average daily demand of 191 MWh.

Chapter 5

Model development and set up

The development of the model is described in this section, along with the set up of the optimization problem.

5.1 Land availability

An energy system based on solar PV is heavily reliant on the land available in the area of system modeling. To estimate the maximum output of solar generation in Djerba, several factors were accounted for. The population of 160,000, the amount of the hotels, the infrastructure, the roads as well service and commercial buildings were taking into place to the total surface area of 517km^2. In this study, it is estimated that 1% of the total surface area can be used to install the proposed energy system. This also include the irregularities that are typical in a land. The 1% results in roughly 5km^2 that can be used to install solar PV modules. With a single solar module of 2m^2, the total surface area could host roughly a total 2.5M solar PV modules. However, this number could be adjusted depending on the number of battery packs and the spacing between the solar modules. This land availability is crucial to later define the maximum capacity of both the solar panels and batteries, which will be discussed in the next chapter.

5.2 Energy system layout

The proposed energy system in study consists of solar PV modules, a battery bank for energy storage and a DC/AC inverter. The solar modules convert sunlight to electricity throughout hours of the day. The dynamics behind this energy system is held to some simplicity. When the solar modules generate electricity that exceeds the demand in each hour, the excess electricity is stored in the battery bank. When the electricity load demand exceeds the solar generation than the battery serves as a generator to meet the demand in each hour. The inverter's job is to convert the DC current from both the solar modules and the battery into AC current that is required from the load.

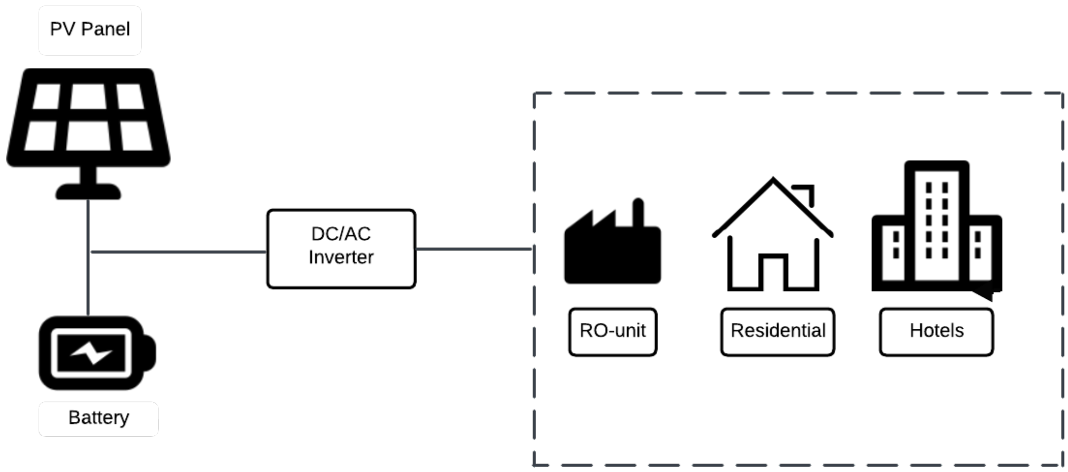

Figure 5.1: Energy system illustration

The layout of this energy system is illustrated in Figure 5.1 which provides a visual representation of the components and their interactions. The demand load in this system consists of the electricity consumption from the RO-unit (water desalination plant), the residential sector and the hotels. The RO-unit is treated as a singular operational unit in this depiction excluding the differences between the consumption between the pumping system and the desalination station.

The configuration of this system offers opportunities to disregard the reliability on the power grid hence making it an off-grid or a stand-alone system. This system can, potentially, serve as a resilient alternative for the fossil fuel-based generation system that is in operation today.

The performance of this system is evaluated on the basis of economic and technical criteria. The economic criteria includes the financial metrics mentioned in 3.3, and the cost effectiveness of the system will be evaluated based on the total system costs and LCOE. For having a reliable system, from a technical point of view, the concept of the loss of power supply probability (LPSP) will be assessed. LPSP is defined by a number between 0 and 1 where 1 means that the load will never be satisfied and 0 means that the load will always be satisfied, see Equation 5.1. This concept is common when evaluating an off-grid solar PV system, and is a great measure to ensure the reliability of the electricity generation as well as meeting the load demand.

$$\text{LPSP} = \frac{\sum_{t=1}^{T} \text{LPS}(t)}{\sum_{t=1}^{T} P_{\text{Load}}(t)} \tag{5.1}$$

where LPS is the loss of power supply.

$$\text{LPS}(t) = P_{\text{Load}}(t) - P_{\text{gen}}(t) \tag{5.2}$$

Scenarios
To analyse the simulation based on the optimization objective, which will be described later in Chapter 5.3, three different scenarios will be elaborated based on different demand loads.

- *Base case scenario* is based on the total demand from the water desalination plant.
- *Scenario 1* will supplement the base case scenario with the demand from the residential sector.
- *Scenario 2* will further extend the two previous scenarios with the demand from hotels.

The layout and description of the steps used to set up the proposed energy system and optimization problem is show in Figure 5.2.

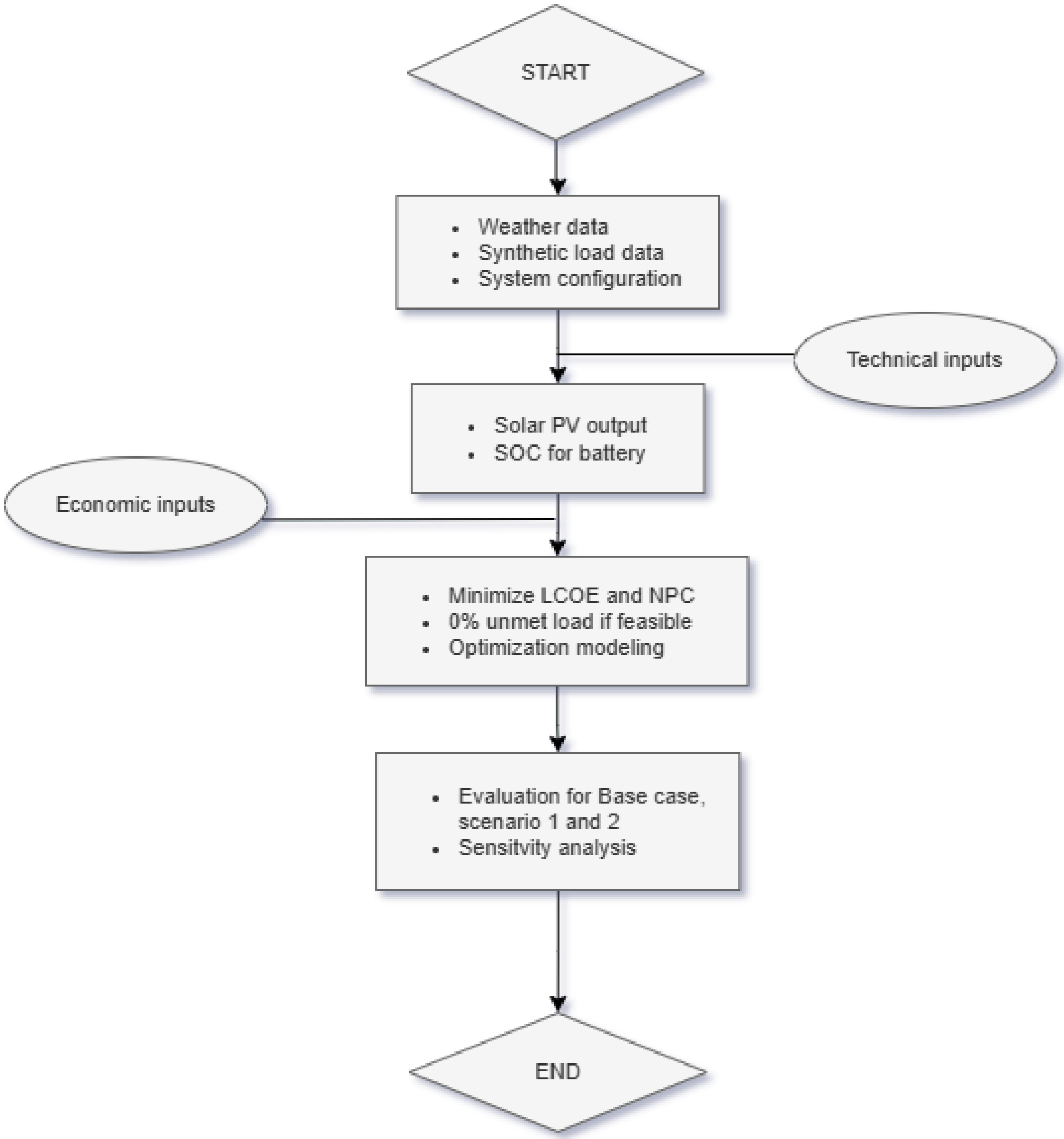

Figure 5.2: Flow chart of the simulation steps

5.2.1 Technical inputs

Table 5.1 represents the technical parameters used for the different components of the energy system. Half-cell monocrystalline solar modules of type AE540MD-144 and lithium-ion batteries module type H48074 are the specific components chosen for this simulation. Their respective sheets can be seen here, [17], [50].

Table 5.1: Technical inputs for the system

Parameters	**Value**	**Unit**
Solar Module		
Nominal maximum power	540	Wp
Module efficiency	20.92	%
Temp. Coefficient	-0.350	%/°C
Nominal operating cell temp.	45	°C
Dimensions	2278 x 1133 x 35	mm
Battery module		
Nominal Capacity	74	Ah
Voltage	48	V
Capacity	3.55	kWh
Depth of Discharge (DOD)	90	%
Efficiency	96	%
Dimensions	442 X 390 X 132	mm

5.2.2 Economic inputs

The economic parameters used in this study are presented in Table 5.2. These are based on findings from the literature review and economic trends in North Africa. [43]

Table 5.2: Economic inputs for the system

Parameters	**Value**	**Unit**
Solar module		
Capital cost	1300	$/kW
O & M cost	195	$/kWh
Lifetime	25	years
Battery module		
Capital cost	1250	$/kW
O & M	32	$/kWh
Lifetime	15	years
Discount rate	10	%

5.3 Building optimization model

An overview of the optimization model aimed at determining the optimal solar PV and battery capacity while ensuring system cost effectiveness, is described below. The model was developed in GAMS, which is a suitable tool for handling large datasets and complex mathematical formulations.

5.3.1 Set definition

To analyze the performance of the simulation, a set comprising all the hours in a day, h = {0,1,2...23}, was used, where $h0$ and $h23$ represent the first and last hour of a day.

5.3.2 Objective Function

The objective function is to minimize the system costs while ensuring the demand is met by the total power generation. Equation 5.3 describes the objective function and includes the capacity of solar PV and battery, the capital and O&M costs, the solar generation and the battery level at hour h.

$$\text{Total\_cost} = C_{\text{pv}} \cdot PV_{\text{cap}} + C_{\text{bat}} \cdot Batt_{\text{cap}} + O_{\text{pv}} \cdot \sum_h E_{\text{pv}}(h) + O_{\text{batt}} \cdot \sum_h E_{\text{batt}}(h) \quad (5.3)$$

5.3.3 Constraints

The objective function is subject to these constraints.

$$\text{SOC}(h) \leq \text{cap\_bat} \quad (5.4)$$

$$\text{SoC}(h) \geq 0 \quad (5.5)$$

$$\text{SoC}(h) \geq \text{SoC\_min} \cdot \text{cap\_bat} \quad (5.6)$$

$$\text{charge}(h) \leq \text{cap\_bat} \cdot \text{max\_c\_rate} \quad (5.7)$$

$$\text{discharge}(h) \leq \text{cap\_bat} \cdot \text{max\_c\_rate} \quad (5.8)$$

$$\text{unmet\_demand}(h) = 0 \quad (5.9)$$

5.3.4 Parameters

The input parameter used in this optimization are:

- Hourly solar output based on the data acquisition done earlier
- Hourly electricity demand for the water desalination plant, residential sector and hotels, augmented according to the different scenarios.
- Ambient temperature acquired from TMY data

5.3.5 Variables

- **pv_output(h)**: Output power of a single PV module at hour h.
- **pv_gen_tot(h)**: Total generated power from the PV system at hour h.
- **cap_pv**: Total installed capacity of the PV system.
- **discharge(h)**: Discharge power from the battery at hour h.
- **charge(h)**: Charge power into the battery at hour h.
- **unmet_demand(h)**: Unmet demand at hour h.
- **SoC(h)**: State of charge of the battery at hour h.
- **system_cost**: Total system cost.

5.3.6 Equations

PV output

$$\mathrm{pv\_gen\_tot}(h) = \mathrm{pv\_output}(h) \cdot \mathrm{cap\_pv} \tag{5.10}$$

Energy balance

$$\mathrm{pv\_gen\_tot}(h) + \frac{\mathrm{discharge}(h)}{\mathrm{batt\_eff}} - \mathrm{charge}(h) \cdot \mathrm{batt\_eff} + \mathrm{unmet\_demand}(h) = \mathrm{demand}(h) \tag{5.11}$$

SOC

$$\mathrm{SoC}(h) = \mathrm{SoC}(h-1) + \mathrm{charge}(h) \cdot \mathrm{batt\_eff} - \frac{\mathrm{discharge}(h)}{\mathrm{batt\_eff}} \quad \forall h > 1 \tag{5.12}$$

Initial SOC

$$\mathrm{SoC(h0)} = \mathrm{initial\_SoC} \cdot \mathrm{cap\_bat} \tag{5.13}$$

Chapter 6

Evaluation of the results

This final part of the study evaluates the proposed results for the optimization problem of the energy system.

6.1 Visualisation of the results

6.1.1 System Architecture

Parts of this study was dedicated to analyzing the possibilities of developing an energy system model based on solar PV and energy storage in a water tank. As the water desalination plant in Djerba was one of the three major electricity consumers, some of the research done in this study was dedicated to energy storage in a water tank. The water desalination plant is a complex set up that contains a lot of pumps and different membranes to convert seawater and brackish water into fresh water. Depending on the size and the technology of the water desalination plant, it can reach up to a 50% conversion rate. Many studies suggested the feasibility of integrating water tanks as an effective form of energy storage. For instance, Maleki et al. (2014) [41], explored the potential of using water storage while including the LPSP concept and an optimization model based on an artificial bee swarm. Among other studies, many suggest that water storage tank is feasible but it is a complex matter that require detailed analysis and correct model set up.

Despite these findings, the integration of water tank energy storage was excluded from this current assessment. The complexities and limitations associated with the dynamics of the water desalination plant resulted in not exploring further of this option. The analysis of the inflow and outflow of the water from the pumps, accurately assessing water consumption from the hotels was one of the reasons behind this decision. In addition to making assumptions about the water costs and the tank size was seemed to be unreasonable to further analyze this energy system model. Despite this, the integration of energy storage as water tank is not what seems to be the cost-effective tool to incorporate into an off grid energy system per now, as the trend for implementing utility scale batteries is getting higher which again has greater potential in terms of cost effectiveness.

The new energy system model set up as described in the previous section was used. Creating a thorough optimization model that serves to minimize system costs, as well as conserving energy reliability, is a challenge. The purpose of this study is to show the dynamics of the battery system in a way that it supplies the power generation from the sun to meet the electricity demand while ensuring a cost effective system cost without overcharging or undercharging the battery. The overall optimization was assessed and is presented in the next section.

6.1.2 Solar resource

The values from the dataset provided on the global solar irradiation are based on global horizontal plane, meaning sun arrays that hits the the surface horizontally. However, to get the maximum power output from the solar module, the optimal tilt and azimuth angle were determined using the plane of array sky diffuse model, which is based on the solar position, latitude and longitude, GHI, DNI, DHI and solar position. With an optimal tilt angle of 33°C and an azimuth angle of 176 °C the solar irradiance on a tilted plane was determined and is illustrated in Figure 6.1. The total annual irradiation on a tilted plane is estimated at 2304 kWh/m^2 with an average of 6.3 kWh/m2 per day. These values surpass the average North African irradiation of 2200 kWh/m2 considered by IRENA [35], and is a reflection on the solar potential in Djerba.

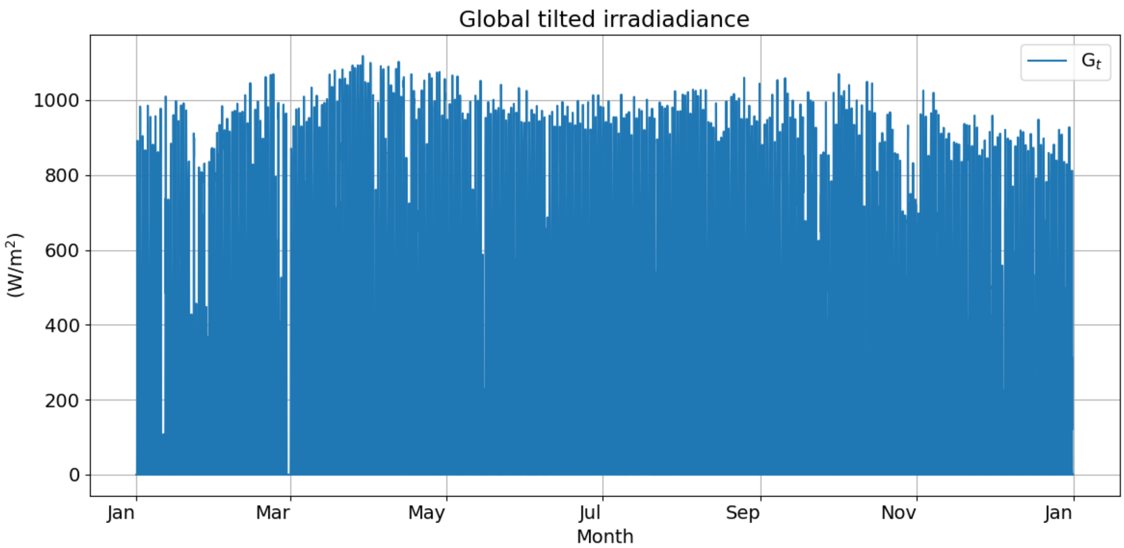

Figure 6.1: Yearly global tilted irradiance (W/m^2)

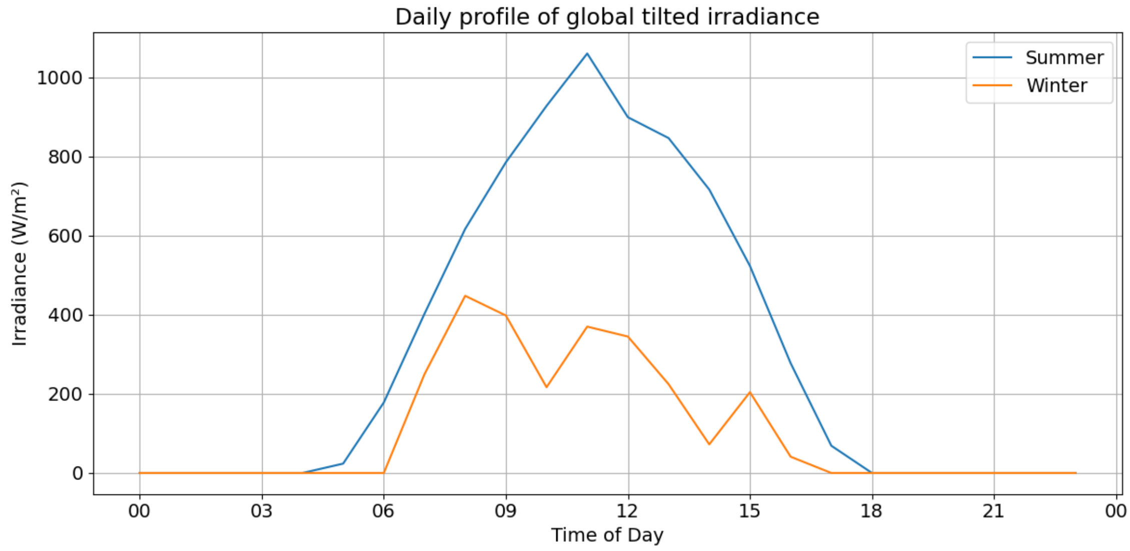

Figure 6.2: Daily summer vs winter global tilted irradiance (W/m^2)

The daily profile illustrated in Figure 6.2, shows the solar potential in Djerba. With a summer peak of over 1000 W/m^2, and considerably good values in the winter. The solar irradiation is stable throughout the year with slight variations between summer and winter times.

6.1.3 Base case scenario

The base case scenario is based on meeting the total electricity demand from the water desalination plant at 43GWh. The optimization model optimizes the capacities of both solar PV modules and battery modules to meet the demand load while minimizing the total cost of the system based on the investment and operation and maintenance cost presented earlier.

The operation dynamics in this system work in a way that the load demand is met by the power from solar PV generation. If there is excess electricity by the solar PV modules then this is stored in the battery. If the solar PV modules cannot meet the demand, then the battery serves as "back up" generator. This ensure the supply reliability of the system to make sure the electricity demand is always met.

The optimization model was conducted in two different parts: a summer day and a winter day. This is done in order to evaluate the behaviour of the proposed energy system in times where solar irradiation is different throughout the day.

Summer

Figure 6.3 represents the PV generation, discharge and charge and the SOC throughout the day in a summer. With a resulted solar capacity of 136 MW, the solar PV module generated enough electricity throughout the day to meet most of the demand. However, from the figure, the battery discharges electricity in the first hours of the day, from 0-5 o'clock. At 5, the solar module start producing electricity reaching a high 73MWh at noon. The excess electricity is stored back in the starting from 09 o'clock and is discharge back after 18. However, the discharges curves behaves in a manner that illustrates the that solar generation cannot meet the demand from each hour at all time. This is mostly due to the optimization model's set up. Since the objective is to minimize the total cost, the optimization model uses the battery, which can be cheaper, in some hours, to meet the demand, and that is what is shown in Figure 6.3. The SOC of the battery starts at 50% of the battery capacity and changes throughout the day with the output of the battery and the variations in the discharge and charge.

The total demand in this base case is met with a total system cost of 840 M$ and a LCOE at 179 $/MWh. These values represent adequate values, compared to the typical LCOE value in Africa explained in the literature review. The NPC cost show good values as well, with respecting the lifetime of both solar PV and batteries. The output results are shown in Table 6.1.

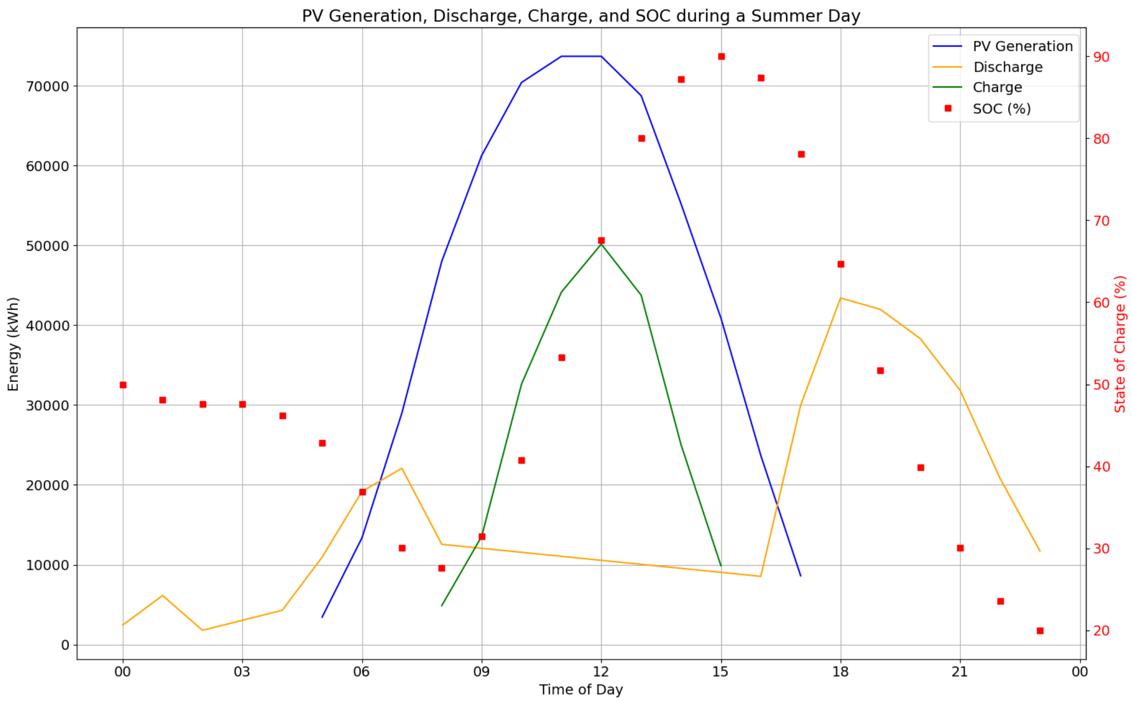

Figure 6.3: Solar PV generation and battery behaviour for a summer day

Parameter	**Value**	**Unit**
Battery capacity	337	MWh
PV capacity	136	MW
System cost	8.4×10^8	$
LCOE	179	$/MWh
NPC	1.8×10^8	$

Table 6.1: Parameter output results for a summer day

Winter

When the energy system is elaborated in a typical winter day, its dynamics change throughout the day. To keep the performance of the energy system through winter day, the battery capacity augmented by 74% compared to the capacity in the summer, see Table 6.2. This is illustrated in Figure **??**, where the PV generation is lower compared to the pv generation in summer. Which is normal due to the lower solar irradiation typically in winter times. This forces the battery to generate more electricity, hence the augmentation of its capacity. This also increases the system cost by just a fraction, the NPC remains the same however the LCOE increases to 230 $/MWh. This is due to the augmentation of the battery generation which affects the overall power generation from the system, which the LCOE is dependent upon.

Parameter	**Value**	**Unit**
Battery capacity	252	MWh
PV capacity	271	MW
System cost	8.5×10^8	$
LCOE	230	$/MWh
NPC	1.8×10^8	$

Table 6.2: Parameter output results for a winter day

The performance of this energy system in the base case scenario show considerable results. The difference between summer and winter capacity is clear, however the total system cost did not seem to change. To evaluate the performance from a technical point of view, it is clear to say that the PV system is substantial enough to meet the electricity demand from the water desalination plant. The batteries are needed in the summer, but mostly in the winter. To further evaluate the performance of this system, it is necessary to see if the system can manage further demand increases.

6.1.4 Scenario 1

In scenario 1, the electricity demand from the residential sector of Djerba was added to the base case scenario. A total of 100 GWh of electricity demand is now to bet met by the proposed system.

Summer

The scenario 1 in a summer day had an improvement in PV and battery capacities with 172 MW and 440 MWh, respectively. This augmentation in capacities demonstrate the feasibility of the energy system to handling an increase in electricity demand and providing sufficient electricity throughout the day. Figure 6.4 illustrated the dynamics of the energy system with a "new" peak of solar PV at 87 MWh, happening at noon. The SOC curves is proportional with the dynamics of the battery which discharges at the beginning and end of the day. Table 6.3

represents the output results. The augmentation of the capacities, to meet the electricity demand for both the residential sector and the water desalination plant, results consequently in the rise of total system cost to 1 B$, which indicates a much higher investment. The LCOE decrease slightly less to 178 $/MWh compared to the base case. The NPC also rises to 230 M$, which is normal due to the necessity of the higher investment in capacities. This system ensures a reliable and sufficient energy supply during summer.

Parameter	Value	Unit
Battery capacity	440	MWh
PV capacity	172	MW
System cost	1×10^9	$
LCOE	178	$/MWh
NPC	2.3×10^8	$

Table 6.3: Parameter output results for scenario 1 - summer day

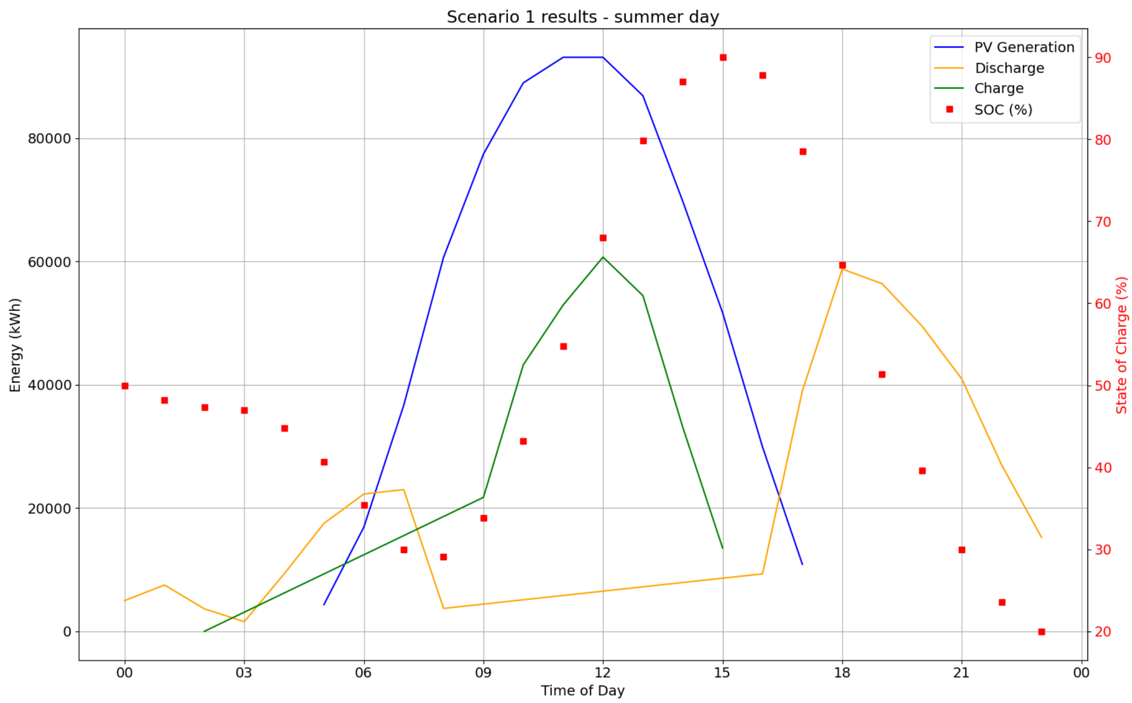

Figure 6.4: Solar PV generation and battery behaviour results from scenario 1 - summer day

Winter

The energy system's performance during winter reflects the solar irradiation throughout the day. In this system, the PV capacity is increased to 380 MW, almost a double from the capacity in the summer. The battery capacity also increases by 74% compared to the base case scenario. This larger capacity of the battery is necessary to store enough electricity to meet the total demand. However, this is directly consequent to the increase in system cost to 1.2 B$. The LCOE also increases to 227 $/MWh, slightly less than the base case, showing that the cost per unit of electricity is higher than in summer but still at competitive levels.

Parameter	Value	Unit
Battery capacity	364	MWh
PV capacity	380	MW
System cost	1.2×10^9	$
LCOE	227	$/MWh
NPC	2.5×10^8	$

Table 6.4: Parameter output results for scenario 1 - winter day

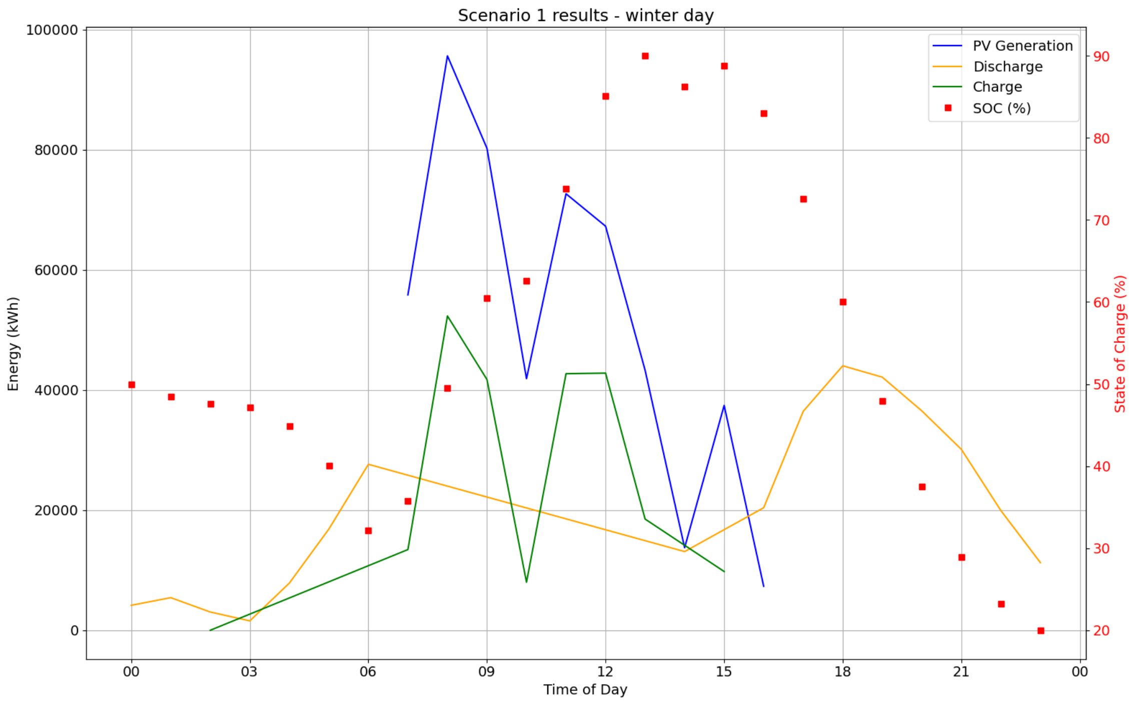

Figure 6.5: Solar PV generation and battery behaviour results from scenario 1 - winter day

6.1.5 Scenario 2

Scenario 2 represents the augmentation of the electricity demand. The load demand from the hotel sector are added to Scenario 1 and the overall energy system is evaluated based on summer and winter days.

Summer

The performance of the energy system based on the total electricity demand throughout a summer day is illustrated in Figure 6.6. Where the solar generation reaches 110 MWh with a capacity of 217. This represents approximately 60% augmentation from the base case. The battery capacity has also increased by 65% to 556 MWh. This expansion is necessary to ensure the power reliability of the energy system during the day and night. The total system cost for this setup reaches 1.3 B$, with an LCOE of 180$/MWh and a NPC of 290 M$.

Parameter	Value	Unit
Battery capacity	556	MWh
PV capacity	217	MW
System cost	1.3×10^9	$
LCOE	180	$/MWh
NPC	2.9×10^8	$

Table 6.5: Parameter outputs results for scenario 2 - summer day

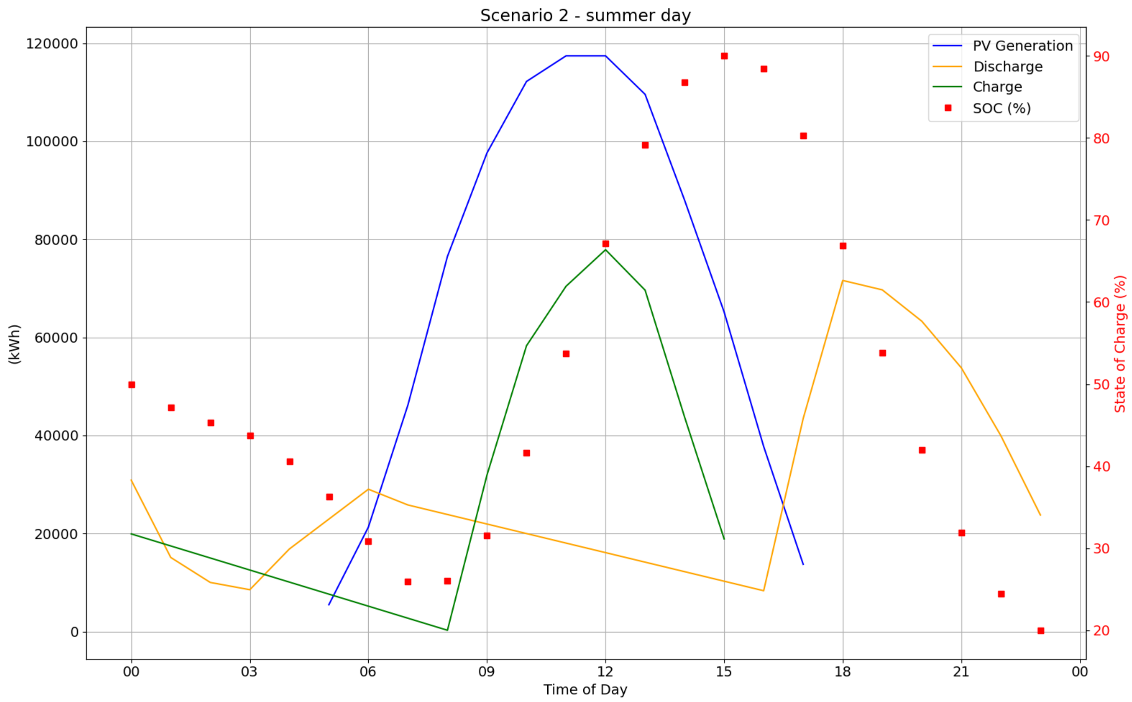

Figure 6.6: Solar PV generation and battery behaviour from Scenario 2 - summer day

Winter

In winter, the energy system's performance is regulated due to the low solar irradiation. This has resulted in an increase of both solar PV and battery capacities. The capacity of solar PV has increased by almost a double, reaching 473 MW. Figure 6.7 illustrates the PV generation and battery dynamics throughout a winter day. The decrease in solar generation has a direct correlation with the increase of battery capacity. Even though the PV modules reach a high 118 MWh generation, this is still not enough to meet the load demand. The battery capacity is then increased by 481 MWh to ensure sufficient energy supply to the system. The increase in capacity results in the increase of the total system cost to In winter, the energy system faces the challenge of 1.5 B$ and a LCOE of 228 $/MWh, with an NPC of 320 M $. Despite the higher costs, this setup guarantees a reliable power supply, even in winter's less favorable solar conditions.

Parameter	**Value**	**Unit**
Battery capacity	481	MWh
PV capacity	473	MW
System cost	1.5×10^9	$
LCOE	228	$/MWh
NPC	3.2×10^8	$

Table 6.6: Parameter output results for scenario 2 - winter day

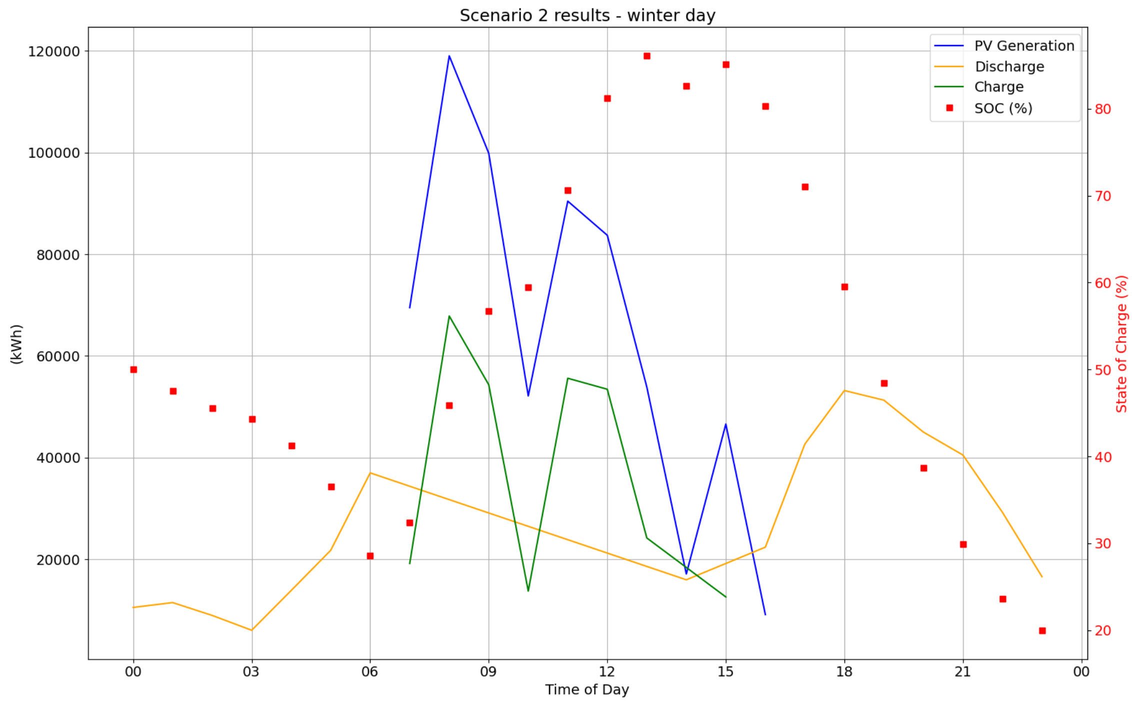

Figure 6.7: Solar PV generation and battery behaviour for scenario 2 - winter day

The proposed energy system demonstrate adaptability and robustness in meeting the electricity demands of the desalination plant and residential and hotel sectors. The energy system ensure power supply throughout the year despite lower solar irradiation in the winter. The 170 GWh demand from scenario 2 is met by augmenting solar PV capacity and especially the capacity of the batteries. The proposed energy system ensures that 56% of Djerba's total electricity demand is met, reducing 453 tons of metric CO^2 yearly. Compared to the findings from literature review the LCOE and NPC from this energy system is considerably good results. The electricity cost is slightly higher than compared to the electricity cost of the water desalination plant.

Considering the uncertainty around generating synthetic data in addition to the model set up the values from these results can serve as an indicator to show the feasibility of integrating renewable energy sources in Djerba. Having reliable power supply at all times are crucial in island and rural areas, with solar PV and batteries this is feasible. However the total system cost are high which reflects the economic part of Africa, where technology trends are more expensive compared to other regions of the world. Integrating this proposed system necessitates in findings investment which can be challenging in Tunisia due the lack of economic reliability.

Chapter 7

Conclusion

This thesis aimed to exploring the potential of solar PV combined with battery storage to meet the electricity demand of Djerba island. Through an extensive literature review, the state of PV was highlighted in North Africa.

In the effort to develop an energy system, a model was developed using GAMS and Python. This model intended to assess the feasibility of integrating solar PV with battery storage to enhance the renewable energy share in Africa through analysis of three scenarios. The performance of the proposed energy system was evaluated and the energy system showed robustness and adaptive to the electricity demand variations. The system can enhance the sustainable reliability while ensuring power supply in Djerba. This reflects the feasibility of solar PV and battery storage on Djerba island.

The proposed energy system not only demonstrates technical feasibility but also highlights economic challenges, particularly in regions like Africa where technology costs are higher. Despite the high total system costs, the integration of renewable energy sources such as solar PV and batteries offers a sustainable and reliable solution for power supply in island and rural areas. However, securing the necessary investment for such projects remains a challenge due to economic constraints in Tunisia.

Overall, the results indicate that while the financial investment is substantial, the benefits of a reliable and sustainable power supply justify the costs. This energy system provides a viable pathway for integrating renewable energy into Djerba's infrastructure, contributing to energy security and environmental sustainability.

Bibliography

[1] Mohammad Ali Abdelkareem, M. El Haj Assad, Enas Taha Sayed, and Bassel Soudan. Recent progress in the use of renewable energy sources to power water desalination plants. *Desalination*, 435:97–113, June 2018. ISSN 0011-9164. doi: 10.1016/j.desal.2017.11.018. URL https://www.sciencedirect.com/science/article/pii/S0011916417321306.

[2] Olivia Agua, Robert Basilio, Mc Erschad Pabillan, Michael Castro, Philipp Blechinger, and Joey Ocon. Decentralized versus Clustered Microgrids: An Energy Systems Study for Reliable Off-Grid Electrification of Small Islands. *Energies*, 13:4454, August 2020. doi: 10.3390/en13174454.

[3] Ephraim Bonah Agyekum. Techno-economic comparative analysis of solar photovoltaic power systems with and without storage systems in three different climatic regions, Ghana. *Sustainable Energy Technologies and Assessments*, 43: 100906, February 2021. ISSN 2213-1388. doi: 10.1016/j.seta.2020.100906. URL https://www.sciencedirect.com/science/article/pii/S2213138820313333.

[4] Tri Ayodha Ajiwiguna, Ga-Ram Lee, Byung-Ju Lim, Sung-Hoon Cho, and Chang-Dae Park. Optimization of battery-less PV-RO system with seasonal water storage tank. *Desalination*, 503:114934, May 2021. ISSN 0011-9164. doi: 10.1016/j.desal.2021.114934. URL https://www.sciencedirect.com/science/article/pii/S0011916421000059.

[5] M. A. Alghoul, P. Poovanaesvaran, M. H. Mohammed, A. M. Fadhil, A. F. Muftah, M. M. Alkilani, and K. Sopian. Design and experimental performance of brackish water reverse osmosis desalination unit powered by 2 kW photovoltaic system. *Renewable Energy*, 93:101–114, 2016. ISSN 0960-1481. doi: https://doi.org/10.1016/j.renene.2016.02.015. URL https://www.sciencedirect.com/science/article/pii/S0960148116301161.

[6] Safa Mahdi Aljabore. Efficiency of Lithium-Ion Battery Energy Storage System. Technical report, Intitute for Technology, 2023. URL https://www.duo.uio.no/bitstream/handle/10852/103807/SafaAljaboreMasterThesis2023.pdf?sequence=11&isAllowed=y.

[7] ANME. Solaire Photovoltaique | ANME, 2023. URL https://anme.tn/fr/content/solaire-photovoltaique.

[8] Ryan Austin. Solar Inverter Efficiency - What is the Most Efficient Solar

Inverter?, October 2017. URL https://understandsolar.com/solar-inverter-efficiency/.

[9] Binson Babu. Self-discharge in rechargeable electrochemical energy storage devices. *Energy Storage Materials*, 67:103261, March 2024. ISSN 2405-8297. doi: 10.1016/j.ensm.2024.103261. URL https://www.sciencedirect.com/science/article/pii/S2405829724000886.

[10] Fazia Baghdadi, Kamal Mohammedi, Said Diaf, and Omar Behar. Feasibility study and energy conversion analysis of stand-alone hybrid renewable energy system. *Energy Conversion and Management*, 105:471–479, November 2015. ISSN 0196-8904. doi: 10.1016/j.enconman.2015.07.051. URL https://www.sciencedirect.com/science/article/pii/S0196890415007025.

[11] Yahia Bakelli, Amar Hadj Arab, and Boubekeur Azoui. Optimal sizing of photovoltaic pumping system with water tank storage using LPSP concept. *Solar Energy*, 85(2):288–294, February 2011. ISSN 0038-092X. doi: 10.1016/j.solener.2010.11.023. URL https://www.sciencedirect.com/science/article/pii/S0038092X10003646.

[12] The World Bank. Solar resource maps of Tunisia - GIS data, 2020. URL https://solargis.com/maps-and-gis-data/download/tunisia. @2020 The World Bank, Source: Global Solar Atlas 2.0, Solar resource data: Solargis.

[13] Maged Bouchahma and Wanglin Yan. Automatic Measurement of Shoreline Change on Djerba Island of Tunisia. *Computer and Information Science*, 5(5): p17, July 2012. ISSN 1913-8989. doi: 10.5539/cis.v5n5p17. URL https://ccsenet.org/journal/index.php/cis/article/view/17716. Number: 5.

[14] L.Carl Brown and Mohammed Talbi. Tunisia - Arabic, French, Berber | Britannica, April 2024. URL https://www.britannica.com/place/Tunisia/Languages.

[15] Ravi Chaurasia, Sanjay Gairola, and Yash Pal. Technical, economic feasibility and sensitivity analysis of solar photovoltaic/battery energy storage off-grid integrated renewable energy system. *Energy Storage*, 4(1):e283, February 2022. ISSN 2578-4862. doi: 10.1002/est2.283. URL https://onlinelibrary.wiley.com/doi/10.1002/est2.283. Publisher: John Wiley & Sons, Ltd.

[16] European Commission. JRC Photovoltaic Geographical Information System (PVGIS) - European Commission, 2024. URL https://re.jrc.ec.europa.eu/pvg_tools/en/.

[17] Solar Power Company. Modules Photovoltaïque – Solar Power Company, 2024. URL https://www.solar-power-company.com/modules-photovoltaique1/.

[18] GAMS Development Corp. GAMS, 2024. URL https://www.gams.com/products/gams/gams-language/.

[19] Dima. Tunisia's Plan for Renewable Energy: Chances and Challenges, March 2023. URL https://fanack.com/economy/features-insights/tunisias-plan-for-renewable-energy-chances-and-challenges~255716/.

[20] Hassen EL AGREBI. Innovative solutions for energy transition in the Tunisian island of Djerba, September 2019. URL https://meetmed.org/wp-content/uploads/2019/05/7THCON1.pdf. 7th MEDENER International Conference.

[21] Slah Farhani, El Manaa Barhoumi, Qamar Ul Islam, and Faouzi Becha. Optimal design and economic analysis of a stand-alone integrated solar hydrogen water desalination system case study agriculture farm in Kairouan Tunisia. *International Journal of Hydrogen Energy*, 63:759–766, April 2024. ISSN 0360-3199. doi: 10.1016/j.ijhydene.2024.03.043. URL https://www.sciencedirect.com/science/article/pii/S0360319924008681.

[22] Kamel Fethi. Desalination in Tunisia - Solar power PV power PV - Case Ben Guerdene Guerdene desalination plant, June 2021. URL https://www.un.org/sites/un2.un.org/files/sonede_desalination_in_tunisia.pdf.

[23] Vasilis Fthenakis, Adam A. Atia, Olivier Morin, Raed Bkayrat, and Parikhit Sinha. New prospects for PV powered water desalination plants: case studies in Saudi Arabia. *Progress in Photovoltaics: Research and Applications*, 24(4): 543–550, 2016. ISSN 1099-159X. doi: 10.1002/pip.2572. URL https://onlinelibrary.wiley.com/doi/abs/10.1002/pip.2572. _eprint: https://onlinelibrary.wiley.com/doi/pdf/10.1002/pip.2572.

[24] Christiania Honsberg and Stuart Bowden. Solar Energy | PVEducation, 2024. URL https://www.pveducation.org/pvcdrom/introduction/solar-energy.

[25] Christiania Honsberg and Stuart Bowden. Storage in PV Systems | PVEducation, 2024. URL https://www.pveducation.org/pvcdrom/batteries/storage-in-pv-systems.

[26] Christiania Honsberg and Stuart Bowden. Summary and Comparison of Battery Characteristics | PVEducation, 2024. URL https://www.pveducation.org/pvcdrom/battery-characteristics/summary-and-comparison-of-battery-characteristics.

[27] IDA. International Desalination and Reuse Association - Homepage, 2024. URL https://idadesal.org/.

[28] IEA. Tunisia - Countries & Regions - Renewable energy, 2021. URL https://www.iea.org/countries/tunisia/renewables.

[29] IEA. Tunisia - Countries & Regions - Energi-mix, 2021. URL https://www.iea.org/countries/tunisia/energy-mix.

[30] IEA. Tunisia - Countries & Regions - Electricity, 2021. URL https://www.iea.org/countries/tunisia/electricity.

[31] IEA. Executive summary – World Energy Outlook 2023 – Analysis, 2023. URL https://www.iea.org/reports/world-energy-outlook-2023.

[32] IEA. Clean Energy Market Monitor – March 2024 – Analysis, March 2024. URL https://www.iea.org/reports/clean-energy-market-monitor-march-2024.

[33] IHEE. Étude d'Impact sur l'Environnement du projet de réalisation de la station de dessalement de l'eau de mer de Jerba de capacité 50 000 m3/jour. Technical Report 24-06, SOCIETE NATIONALE D'EXPLOITATION ET DE DISTRIBUTION DES EAUX, 8, Rue Hbib Chrita Ariana, April 2015. URL https://www.sonede.com.tn/accueil/contenu-principal/acces-a-linformation/documents-accessibles.

[34] IRENA. Planning and prospects for renewable power: North Africa. Technical report, Energy Department, 2023. URL https://www.irena.org/Publications/2023/Jan/Planning-and-prospects-for-renewable-power-North-Africa.

[35] IRENA and AfDB. Renewable Energy Market Analysis: Africa and Its Regions. Technical report, Energy Department, January 2022. URL https://www.irena.org/publications/2022/Jan/Renewable-Energy-Market-Analysis-Africa.

[36] Marc Korevaar. Measuring Solar Irradiance for Photovoltaics. In *Measuring Solar Irradiance for Photovoltaics*. -, August 2022. ISBN 978-1-83968-858-4. doi: 10.5772/intechopen.105580.

[37] Eftichios Koutroulis, Dionissia Kolokotsa, Antonis Potirakis, and Kostas Kalaitzakis. Methodology for optimal sizing of stand-alone photovoltaic/wind-generator systems using genetic algorithms. *Solar Energy*, 80 (9):1072–1088, September 2006. ISSN 0038-092X. doi: 10.1016/j.solener.2005.11.002. URL https://www.sciencedirect.com/science/article/pii/S0038092X05003713.

[38] Senthil Kumarasamy, Shankar Narasimhan, and Sridharakumar Narasimhan. Optimal operation of battery-less solar powered reverse osmosis plant for desalination. *Desalination*, 375:89–99, November 2015. ISSN 0011-9164. doi: 10.1016/j.desal.2015.07.029. URL https://www.sciencedirect.com/science/article/pii/S0011916415300370.

[39] Tom Lambert, Paul Gilman, and Peter Lilienthal. Micropower System Modeling with Homer. In Felix A. Farret and M. Godoy Simões, editors, *Integration of Alternative Sources of Energy*, pages 379–418. Wiley, 1 edition, December 2005. ISBN 978-0-471-71232-9 978-0-471-75562-3. doi: 10.1002/0471755621.ch15. URL https://onlinelibrary.wiley.com/doi/10.1002/0471755621.ch15.

[40] Laurea Magistrale. Modelling, Simulation and Analysis of the Tunisian Power System. Technical report, Collegio di Ingegneria Energetica, October 2018. URL https://webthesis.biblio.polito.it/secure/8726/1/tesi.pdf.

[41] Akbar Maleki and Alireza Askarzadeh. Artificial bee swarm optimization for optimum sizing of a stand-alone PV/WT/FC hybrid system considering LPSP concept. *Solar Energy*, 107:227–235, September 2014. ISSN 0038-092X. doi: 10.1016/j.solener.2014.05.016. URL https://www.sciencedirect.com/science/article/pii/S0038092X1400245X.

[42] Aishwarya S. Mundada, Kunal K. Shah, and J. M. Pearce. Levelized cost of electricity for solar photovoltaic, battery and cogen hybrid systems. *Renewable and Sustainable Energy Reviews*, 57:692–703, May 2016. ISSN 1364-0321. doi: 10.1016/j.rser.2015.12.084. URL https://www.sciencedirect.com/science/article/pii/S1364032115014677.

[43] ATB NREL. Utility-Scale Battery Storage | Electricity | 2022 | ATB | NREL, 2023. URL https://atb.nrel.gov/electricity/2022/utility-scale_battery_storage.

[44] Ramia Ouederni, Bechir Bouaziz, and Faouzi Bacha. Design and evaluation of an island's hybrid renewable energy system in Tunisia. In *2022 5th International Conference on Advanced Systems and Emergent Technologies (IC_ASET)*, pages 418–423, Hammamet, Tunisia, March 2022. IEEE. ISBN 978-1-66542-735-7. doi: 10.1109/IC_ASET53395.2022.9765903. URL https://ieeexplore.ieee.org/document/9765903/.

[45] Arthur Leandro Guerra Pires, Paulo Rotella Junior, Luiz Célio Souza Rocha, Rogério Santana Peruchi, Karel Janda, and Rafael de Carvalho Miranda. Environmental and financial multi-objective optimization: Hybrid wind-photovoltaic generation with battery energy storage systems. *Journal of Energy Storage*, 66:107425, August 2023. ISSN 2352-152X. doi: 10.1016/j.est.2023.107425. URL https://www.sciencedirect.com/science/article/pii/S2352152X23008228.

[46] HOMER Pro. Creating a Synthetic Load from a Profile, 2024. URL https://support.ul-renewables.com/homer-manuals-pro/creating_a_synthetic_load_from_profile.html.

[47] UN Environment programme. The Sectoral Solution to Climate Change, 2023. URL https://www.unep.org/interactive/six-sector-solution-climate-change/.

[48] Bijan Rahimi, Hamed Shirvani, Ali Asghar Alamolhoda, Fathollah Farhadi, and Mohammadreza Karimi. A feasibility study of solar-powered reverse osmosis processes. *Desalination*, 500:114885, March 2021. ISSN 0011-9164. doi: 10.1016/j.desal.2020.114885. URL https://www.sciencedirect.com/science/article/pii/S0011916420315630.

[49] Vendoti Suresh, Muralidhar M., and R. Kiranmayi. Modelling and optimization of an off-grid hybrid renewable energy system for electrification in a rural areas. *Energy Reports*, 6:594–604, November 2020. ISSN 2352-4847. doi: 10.1016/j.egyr.2020.01.013. URL https://www.sciencedirect.com/science/article/pii/S2352484718304499.

[50] Pylon Technologies. Powercube H2 energy storage system-Pylon Technologies Co., Ltd., 2024. URL https://en.pylontech.com.cn/pro_detail.aspx?id=128&cid=24.

[51] Davide Trapani, Paolo Marocco, Domenico Ferrero, Karen Byskov Lindberg, Kyrre Sundseth, and Massimo Santarelli. The potential of hydrogen-battery storage systems for a sustainable renewable-based electrification of remote islands in Norway. *Journal of Energy Storage*, 75:109482, January 2024. ISSN 2352-152X. doi: 10.1016/j.est.2023.109482. URL https://www.sciencedirect.com/science/article/pii/S2352152X23028803.

[52] E. Tzen, D. Theofilloyianakos, and Z. Kologios. Autonomous reverse osmosis units driven by RE sources experiences and lessons learned. *Desalination*, 221 (1):29–36, February 2007. ISSN 0011-9164. doi: 10.1016/j.desal.2007.02.048. URL https://www.sciencedirect.com/science/article/pii/S0011916407006765.

[53] UNDP. DREI Tunisia, 2018. URL https://www.undp.org/energy/publications/drei-tunisia.

[54] UNFCC. The Paris Agreement | UNFCCC, 2015. URL https://unfccc.int/process-and-meetings/the-paris-agreement.

[55] Our world in Data. Population, 2022. URL https://ourworldindata.org/grapher/population?tab=chart&country=~TUN.

[56] Salman Zafar. Solar Energy in Tunisia | EcoMENA, July 2023. URL https://www.ecomena.org/solar-tunisia/.

Appendix A

Appendix: Consumption data

1. Présentation de la station

La station de dessalement d'eau de mer de Djerba est officiellement entrée en fonction le 02 mai 2018 après 5 ans de construction constituant la première station de dessalement d'eau de mer en Tunisie.

Figure 1 : localisation Station de dessalement de l'eau de mer de Djerba

Ce projet a pour but de couvrir les besoins en eau potable de 175 000 habitants dans l'ile de Djerba (y compris les hôtels) à 100% jusqu'à 2035 et en plus de fournir 20 000 m3/J aux régions de Zarzis, Ben Guerdane, Médenine et Tataouine vers l'année 2023.

Actuellement la station produit quotidiennement 60 000 m3 d'eau douce de salinité 1.4 g/l dont 50 000 provient de l'eau osmosée et 10 000 provient de l'eau de forage qui se mélange avec l'eau douce lors de la reminéralisation.

2. Processus de dessalement de l'eau de mer

Le circuit du dessalement de la station de Djerba fonctionne comme suit :

❖ Le captage de l'eau de mer à partir d'une profondeur de 12m et son acheminement vers la station de traitement distante du point de prise d'eau de 2.4 km.

❖ L'eau de mer pompée subit un prétraitement qui consiste à éliminer les matières en suspension présentes dans l'eau en utilisant un dégrillage et une filtration sous un filtre à cartouche plus fine.

❖ Ensuite l'eau traverse un bloc d'osmose inverse permettant la séparation de

L'eau douce de celle saumâtre sous une pression de 62.7 bars à travers des membranes semi-perméable (deux lignes d'osmose inverse produisant chacune 25 000 m3) avec un taux de conversion de 46%. Il s'agit de deux étages intégrés de tubes d'osmose dont chaque tube est formée de 8 membranes.

3) Consommation d'énergie électrique pour la station de dessalement d'eau de mer de Djerba et la station de captage d'eau de mer de Djerba

Référence STEG	Stations /Forage ***Site des autres consommateurs***	Gouvernorat
957854	*STATION DE DESSALEMENT D'EAU DE MER DE JERBA*	*MEDENINE*
957360	*SONEDE ST DE CAPTAGE D'EAU DE MER DE JERBA*	

3.1 Consommations d'énergie électrique et coût pour les stations citées au tableau ci-dessus

- STATION DE DESSALEMENT D'EAU DE MER DE JERBA (Ref STEG 957854)

	Consommation d'énergie électrique en kWh			
Mois/année	2020	2021	2022	2023
Janvier	1934336	1787047	1791568	2469624
Février	1591836	1715801	2087214	1892311
Mars	1858998	1841309	1937221	2605492
Avril	2014793	2378683	3212494	3270808
Mai	2528586	2624215	3822205	2970580
Juin	3378357	3405347	3445873	3074063
Juillet	3315586	3465265	3183180	3809795
Août	3560182	3505356	3914767	3694807
Septembre	2743957	3655281	2763762	3422673
Octobre	2300756	2491517	3085665	3553008
Novembre	2418870	2096128	3456572	3212888
Décembre	1571398	2179990	2923728	2657192
Total annuel	**29 217 655**	**31 145 939**	**35 624 249**	**36 633 241**

- *SONEDE ST DE CAPTAGE D'EAU DE MER DE JERBA* (Ref STEG 957360)

	Consommation d'énergie électrique en kWh			
Mois/année	2020	2021	2022	2023
Janvier	318726	318183	333840	419868
Février	275936	341615	372698	335646
Mars	294506	293269	385503	480013
Avril	341031	399798	480262	602884
Mai	409045	487857	593782	547808
Juin	572611	620328	738743	555665
Juillet	561128	632712	594277	679157
Août	642269	658208	753357	677771
Septembre	562415	545847	484627	637871
Octobre	400441	472569	585575	658783
Novembre	428924	376918	636187	589150
Décembre	290687	381297	548852	491429
Total annuel	**5 097 719**	**5 528 601**	**6 507 703**	**6 676 045**

3.2 Consommation d'énergie électrique mensuelle pour la stations de dessalement d'eau de mer de Jerba et le station de captage d'eau de mer de Jerba

Désignation	**Unité**	2020	2021	2022	2023
Consommation d'énergie électrique	GWh	*34,32*	*36,67*	*42,13*	*43,31*
Coût d'énergie électrique TTC	MD	*10,37*	*11,00*	*13,46*	*15,12*